

UV Transmission in Natural Waters on Prebiotic Earth

S. Ranjan^{1,2,3,*}, C. L. Kufner⁴, G. G. Lozano⁴, Z. R. Todd^{4,5}, A. Haseki^{1,6}, D. D. Sasselov⁴

¹Massachusetts Institute of Technology, Department of Earth, Atmospheric & Planetary Sciences,
Cambridge, MA 02139

²Northwestern University, Center for Interdisciplinary Exploration and Research in Astrophysics &

Department of Physics and Astronomy, Evanston, IL 60601

³Blue Marble Space Institute of Science, Seattle, WA 98154

⁴Harvard-Smithsonian Center for Astrophysics, Cambridge, MA 02138

⁵University of Washington, Seattle, WA 98195

⁶Harvard College, Cambridge, MA 02138

*SCOL Postdoctoral Fellow

arXiv:2110.00432v1 [astro-ph.EP] 1 Oct 2021

Corresponding author: Sukrit Ranjan, sukrit.ranjan@northwestern.edu

Abstract

Ultraviolet (UV) light plays a key role in surficial theories of the origin of life, and numerous studies have focused on constraining the atmospheric transmission of UV radiation on early Earth. However, the UV transmission of the natural waters in which origin-of-life chemistry (prebiotic chemistry) is postulated to have occurred is poorly constrained. In this work, we combine laboratory and literature-derived absorption spectra of potential aqueous-phase prebiotic UV absorbers with literature estimates of their concentrations on early Earth to constrain the prebiotic UV environment in marine and terrestrial natural waters, and consider the implications for prebiotic chemistry. We find that prebiotic freshwaters were largely transparent in the UV, contrary to assumptions by some models of prebiotic chemistry. Some waters, e.g., high-salinity waters like carbonate lakes, may be deficient in shortwave (≤ 220 nm) UV flux. More dramatically, ferrous waters can be strongly UV-shielded, particularly if the Fe^{2+} forms highly UV-absorbent species like $\text{Fe}(\text{CN})_6^{4-}$. Such waters may be compelling venues for UV-averse origin-of-life scenarios, but are unfavorable for some UV-dependent prebiotic chemistries. UV light can trigger photochemistry even if attenuated through photochemical transformations of the absorber (e.g., e_{aq}^- production from halide irradiation), which may have both constructive and destructive effects for prebiotic syntheses. Prebiotic chemistries invoking waters containing such absorbers must self-consistently account for the chemical effects of these transformations. The speciation and abundance of Fe^{2+} in natural waters on early Earth is a major uncertainty, and should be prioritized for further investigation as it plays a major role in UV transmission in prebiotic natural waters.

Keywords: Prebiotic Earth; Prebiotic Chemistry; Ultraviolet Spectroscopy; Planetary Environments; UV Radiation; Origin of Life

1 Introduction

A key challenge for origin-of-life studies is constraining the range of environmental conditions on early Earth under which life arose. Knowledge of these environmental conditions informs development of theories of the origin of life, and enables assessment of the plausibility and probability of postulated prebiotic chemistries (Pace, 1991; Cleaves, 2013; Barge, 2018; Lyons et al., 2020). Consequently, considerable work has been invested to constrain the range of physico-chemical conditions available in prebiotic environments (Sleep, 2018; Sasselov et al., 2020).

An important prebiotic environmental factor, particularly for surficial prebiotic chemistry, is the ultraviolet (UV) irradiation environment. UV photons can destroy nascent biomolecules, motivating a search for mechanisms to protect prebiotically important molecules from UV irradiation (Sagan, 1973; Holm, 1992; Cleaves & Miller, 1998). On the other hand, UV light has also been suggested to be essential to the origin of life, as a source of chemical free energy and selectivity (Deamer & Weber, 2010; Pascal, 2012; Beckstead et al., 2016). Indeed, UV light has been experimentally shown to drive a range of prebiotic chemistries (Ferris & Orgel, 1966; Sagan & Khare, 1971; Flores et al., 1977; Bonfio et al., 2017; Pestunova et al., 2005; Mariani et al., 2018; J. Xu et al., 2020). Surficial prebiotic chemistries therefore broadly fall into two classes: those for which UV light is strictly destructive and must be mitigated or avoided, and those for which UV light is essential and must be sought (Ranjan & Sasselov, 2016; Todd et al., 2020). The self-consistent availability of UV radiation is consequently a crucial part of the assessment of the plausibility of proposed prebiotic chemistries.

The pivotal roles that UV radiation plays in diverse prebiotic chemistries have motivated increasingly sophisticated estimates of the prebiotic UV environment, with particular emphasis on atmospheric transmission. Models generally predict abundant steady-state UV at wavelengths $\gtrsim 204$ nm and a shortwave cutoff of ≈ 200 nm driven by at-

atmospheric CO₂ and H₂O, though transient eras of low UV are possible after large volcanic eruptions and possibly impacts (Cockell, 2000; Rugheimer et al., 2015; Ranjan & Sasselov, 2017; Ranjan et al., 2018; Zahnle et al., 2020). However, prebiotic chemistry is generally proposed to occur in aqueous reservoirs like ponds or oceans, which may host UV-blocking compounds of geological origin (Martin et al., 2008; McCollom, 2013; Patel et al., 2015; Benner et al., 2019; Becker et al., 2019). To date, estimates of UV transmission in prebiotic natural waters are generally based on pure water or modern pond water (Cockell, 2000; Ranjan & Sasselov, 2016; Pearce et al., 2017).

Neither modern pond water nor pure water are likely representative of prebiotic waters. The UV-opacity of modern pond waters is largely driven by biogenic dissolved carbon species (Morris et al., 1995; Markager & Vincent, 2000; Laurion et al., 2000). In the limit of low biological productivity, as expected on a prebiotic world, natural waters can be clear down to 300 nm; their transmission from 200-300 nm is unconstrained, but has been extrapolated to be similarly low (Smith & Baker, 1981; Morel et al., 2007). At the other extreme, while pure water is clear in the near-UV (Quickenden & Irvin, 1980), the waters in which prebiotic chemistry occurred must by definition have been impure, since they must have contained at minimum the feedstocks for that chemistry, and likely other geogenic constituents as well (e.g., Toner & Catling 2020). Absorption due to these constituents may influence UV transmission. The UV transmission of prebiotic waters therefore likely lies in between the extremes of high transparency and high opacity represented by the previously-utilized proxies of pure water and modern pond water.

In this paper, we constrain wavelength-dependent UV transmission in prebiotic waters. We focus on absorption due to a subset of UV-active species which have been proposed to be present in prebiotic waters. We derive molar absorptivities of these compounds from a combination of literature reports and our own measurements. We draw on literature proposals for the concentrations of these species in representative prebiotic waters. We do not attempt self-consistent geochemical modelling of these waters; such work is important but requires improved measurements of the relevant reaction kinetics under prebiotically relevant conditions, which is beyond the scope of this work. Our work is similar in spirit to the work of Cockell (2000, 2002), who drew on literature proposals for the composition of the prebiotic atmosphere to constrain its UV transmission, without attempting to model its self-consistent photochemistry. Their simple initial analysis guided prebiotic chemistry (e.g., Pierce et al. 2005; Gómez et al. 2007) and motivated more atmospherically sophisticated follow-up work (e.g., Rugheimer et al. 2015), which came to largely similar conclusions. Similarly, we hope our simple study will guide prebiotic chemistry while motivating more geochemically sophisticated follow-up work.

2 Background

Relatively few studies constrain the UV transmission of prebiotic natural waters specifically. A notable exception is Cleaves & Miller (1998), who considered potential "sunscreens" for the prebiotic ocean. Cleaves & Miller (1998) measured the UV absorptivities of salts, HCN and spark-discharge-derived polymers, HS⁻, and marine Fe²⁺. Based on a combination of calculated and literature estimates of the concentrations of these species, Cleaves & Miller (1998) concluded that in favorable circumstances, HS⁻, marine Fe²⁺, or spark discharge polymer could have extinguished UV in the surface layer of the prebiotic ocean. The conditions required for accumulation of spark-discharge polymer to high concentrations in the prebiotic ocean included the emission of prebiotic volcanic carbon as CH₄, its conversion with unity efficiency to spark-discharge polymer, and its efficient deposition to the ocean. However, more recent modelling indicates volcanogenic carbon was emitted even in early Earth-like planets as CO₂, not CH₄, and that the primary fate of abiotic CH₄ should have been oxidation to CO₂ (Kasting, 2014), suggesting the conditions required for accumulation of optically-relevant concentrations of spark discharge polymers were unlikely to be met in the steady state, though high hydrocar-

bon concentrations may be transiently possible after large impacts (Genda et al., 2017; Benner et al., 2019; Zahnle et al., 2020). Similarly, more recent work suggests the early ocean was ferruginous (Fe^{2+} -rich), and would have titrated out HS^- as pyrite; combined with the low solubility of HS^- , $[\text{HS}^-]$ was most likely very low in most natural waters on early Earth (Walker & Brimblecombe, 1985; Poulton & Canfield, 2011; Ranjan et al., 2018). However, elevated $[\text{Fe}^{2+}]$ remains possible for the early ocean (Konhauser et al., 2017).

3 Methods

3.1 Calculating Aqueous UV Attenuation

We approximate the transmission of UV radiation in homogenous (well-mixed), non-scattering aqueous solutions at low concentrations and low light intensities by the Beer-Lambert Law (IUPAC, 1997):

$$\log_{10}(I(\lambda)/I_0(\lambda)) = \log_{10}(T(\lambda)) = -(\sum_i \epsilon_i(\lambda)c_i)d = -(\sum_i a_i(\lambda))d, \quad (1)$$

where I_0 is the incident irradiance, I is the transmitted irradiance, T is the fraction of transmitted radiation, ϵ_i is the molar decadic absorption coefficient for the i th component of the solution, c_i is the concentration of the i th component of the solution, $a = \epsilon c$ is the linear decadic absorption coefficient, and d is the path length. This approach considers only absorption and neglects scattering. This is a reasonable approximation because in the 200–300 nm wavelength range we focus on, the single-scattering albedo of liquid water $\omega_0 \ll 1$, i.e. absorption dominates scattering (Fig. A1; Quickenden & Irvin 1980; Kröckel & Schmidt 2014). We follow previous workers in assuming that ϵ_i does not vary as a function of pH for the simple inorganic molecules we consider, i.e. that changes in the absorbance of solutions of these molecules with pH are due to changes in speciation or complexation, not intrinsic changes to ϵ_i (Braterman et al., 1983; Anbar & Holland, 1992; Nie et al., 2017; Tabata et al., 2021). We propagate the uncertainties on ϵ_i under the assumption that they are independent and normally distributed (Bevington & Robinson, 2003).

3.2 Molar Decadic Absorption Coefficients for Potential Prebiotic Absorbers

We consider absorption due to halide anions (Cl^- , Br^- , I^-), ferrous iron species (Fe^{2+} , $\text{Fe}(\text{CN})_6^{4-}$), sulfur species (HS^- , HSO_3^- , SO_3^{2-}), dissolved inorganic carbon (HCO_3^- , CO_3^{2-}) and nitrate (NO_3^-). Halides are ubiquitous in natural waters on modern Earth due to their high solubility and robust geological source, and hence are thought to have been present in natural waters on early Earth as well (Knauth, 2005; Marty et al., 2018; Hanley & Koga, 2018; Toner & Catling, 2020). Ferrous iron is inferred on early Earth on the basis of banded iron formations (Walker & Brimblecombe, 1985; Li et al., 2013; Konhauser et al., 2017; Toner & Catling, 2019). Dissolved inorganic carbon is inevitable in natural waters on early Earth due to dissolution of atmospheric CO_2 (Krissansen-Totton et al., 2018; Kadoya et al., 2020). Sulfur species may have been present on early Earth due to dissolution of volcanically outgassed sulfur species (Walker & Brimblecombe, 1985; Ranjan et al., 2018). Nitrate is predicted to accumulate in natural waters on early Earth as a product of lightning in an N_2 - CO_2 atmosphere (Mancinelli & McKay, 1988; Wong et al., 2017; Laneuville et al., 2018; Ranjan et al., 2019).

We draw on both the literature and our own measurements for the molar decadic absorption coefficients of potential prebiotic aqueous-phase absorbers. We use our own measurements when available, because our measurements typically feature broader wavelength coverage than the literature, include estimates of uncertainty, and are collected using uniform techniques (Appendix B1). For the ferrous iron species, we check that the dominant ion speciation does not vary due to pH drift over the course of our dilutions

(Appendix B14). Our measurement techniques are potentially inaccurate for weak acids and bases because we do not control pH, which may drift during dilution steps, affecting speciation. For such species, we rely instead on literature data (Appendix B3). Table 1 summarizes the sources of the molar decadic absorption coefficients used in this work.

Table 1. Molar decadic absorption coefficients used in this work

Species	Source
Br^-	As NaBr, this work
Cl^-	As NaCl, this work
I^-	As NaI and KI, this work
NO_3^-	As NaNO_3 , this work
Fe^{2+}	As $\text{Fe}(\text{BF}_4)_2$, this work
$\text{Fe}(\text{CN})_6^{4-}$	As $\text{K}_4\text{Fe}(\text{CN})_6$, this work
HS^-	Guenther et al. (2001)
HSO_3^-	Fischer & Warneck (1996); Beyad et al. (2014)
SO_3^{2-}	Fischer & Warneck (1996); Beyad et al. (2014)
HCO_3^-	Birkmann et al. (2018)
CO_3^{2-}	Birkmann et al. (2018)
H_2O	Quickenden & Irvin (1980)

3.3 Abundances of Potential Prebiotic Absorbers in Fiducial Prebiotic Waters

Constraining the impact of potential absorbers on prebiotic aqueous transmission requires estimates of their abundances in natural waters on early Earth. Natural waters are diverse, and we cannot hope to explore this full diversity. Instead, we focus on fiducial waters motivated by proposed origin-of-life scenarios. We focus primarily on shallow terrestrial waters, e.g. ponds and lakes. Such waters are of interest for prebiotic chemistry because of their propensity for wet-dry cycles, the ability to accumulate atmospherically-delivered feedstocks more efficiently than the oceans, and their potentially diverse palette of environmental conditions (Patel et al., 2015; Deamer & Damer, 2017; Pearce et al., 2017; Becker et al., 2018; Rimmer & Shorttle, 2019; Ranjan et al., 2019; Toner & Catling, 2020). We specifically consider freshwater lakes, carbonate lakes, and ferrocyanide lakes. We also consider the early ocean, to offer a basis of comparison for the terrestrial waters. Our oceanic calculations may also be relevant to origin-of-life scenarios that invoke shallow waters at the land-ocean interface (Commeyras et al., 2002; Lathe, 2005; Bywater & Conde-Frieboes, 2005), but are not relevant to deep-sea origin of life scenarios (e.g., Corliss et al. 1981; Sojo et al. 2016), where water alone is enough to extinct UV. The composition of these waters are uncertain: we draw on the literature to construct high and low transmission endmember cases, to bound their potential UV transmission. Our construction of these endmember cases is summarized in Table 2, and detailed in Sections 3.3.1-3.3.4.

3.3.1 Ocean

For halide species, we scale the composition of the modern oceans. We consider a salinity range of 0.5–2× modern, motivated by theoretical arguments and isotopic evidence (Knauth, 2005, 1998; Marty et al., 2018). On modern Earth, seawater halide concentrations are $[\text{Cl}^-]=0.6\text{M}$, $[\text{Br}^-]=0.9\text{ mM}$, and $[\text{I}^-]=0.5\text{ }\mu\text{M}$ (Channer et al., 1997; ASTM,

Table 2. Estimated range of concentrations of potential prebiotic absorbers in prebiotic waters

Species	Ocean		Freshwater	Pond	Carbonate	Lake	Ferrous	Lake
	Low	High	Low	High	Low	High	Low	High
Br ⁻	0.45 mM	1.8 mM	0.15 μ M	0.15 μ M	1 mM	10 mM	0.15 μ M	0.15 μ M
Cl ⁻	0.3 M	1.2 M	0.2 mM	0.2 mM	0.1 M	6M	0.2 mM	0.2 mM
I ⁻	0.25 μ M	1 μ M	40 nM	600 nM	40 nM	600 nM	40 nM	600 nM
Fe ²⁺	1 nM	0.1 mM	0.1 μ M	0.1 mM	0	0	0	0
Fe(CN) ₆ ⁴⁻	0	0	0	0	0	0	0.1 μ M	0.1 mM
NO ₃ ⁻	2×10^{-15} M	0.5 μ M	0.05 nM	10 μ M	5 nM	1 mM	0.05 nM	10 μ M
HS ⁻	0	0	0	8×10^{-11} M	0	8 nM	0	8×10^{-11} M
HSO ₃ ⁻	0	0	0	200 μ M	0	200 μ M	0	200 μ M
SO ₃ ²⁻	0	0	0	100 μ M	0	400 μ M	0	100 μ M
HCO ₃ ⁻	2 mM	0.2M	1 mM	1 mM	50 mM	0.1 M	1 mM	1 mM
CO ₃ ²⁻	0.2 μ M	1 mM	100 nM	100 nM	7 μ M	7 mM	100 nM	100 nM

2013). Cl⁻ and Br⁻ covary in natural waters, leading us to fix their prebiotic ratios to the modern value (Hanley & Koga, 2018). De Ronde et al. (1997) used fluid inclusions to infer high [I⁻] at 3.2 Ga, but the interpretation of these samples is strongly contested (Lowe & Byerly, 2003; Knauth, 2005; Farber et al., 2015). We therefore fix our prebiotic [I⁻]/[Cl⁻] to the modern value as well, and assume these ions to covary in the prebiotic ocean.

Estimates of ferrous iron concentrations in the surficial prebiotic ocean vary significantly. Halevy et al. (2017) estimate [Fe²⁺] < 10⁻⁹M in the surface ocean, largely driven by the assumption of efficient photooxidation. More recent work reports this process to be less efficient and estimates [Fe²⁺] = 10⁻⁴M in the surface ocean (Konhauser et al., 2007; Halevy & Bachan, 2017; Konhauser et al., 2017). Fe²⁺ is predicted to be the main ferrous species at circumneutral pH for solutions with oceanic Cl⁻ and SO₄²⁻ concentrations in equilibrium with 0.03 atm CO₂, which approximates conditions for the Archaean ocean (King, 1998; Halevy & Bachan, 2017; Krissansen-Totton et al., 2018). We therefore assume the ferrous iron to be present as Fe²⁺, and we adopt 10⁻⁹M and 10⁻⁴M as our bracketing estimates for [Fe²⁺] in the photic zone.

We take the bracketing range of oceanic [NO₃⁻] from Ranjan et al. (2019). We take oceanic sulfide concentrations to be negligible due to titration with Fe²⁺ (Walker & Brimblecombe, 1985; Poulton & Canfield, 2011). We take oceanic sulfite and bisulfite concentrations to be negligible (Halevy, 2013). We take bracketing oceanic carbonate and bicarbonate concentrations spanning the range at 3.9 Ga defined by "standard" and "control" cases of the early ocean model of Kadoya et al. (2020).

3.3.2 Freshwater Lakes

Terrestrial waters are typically dilute, with ionic strength of order 10⁻³ M (Lerman et al., 1995). To represent a dilute endmember scenario for natural waters, we consider freshwater lakes with riverine composition (i.e., not evaporatively concentrated). Modern surface freshwater systems average [Cl⁻] = 0.2 mM, and the same is proposed for Archaean and prebiotic river waters (Graedel & Keene, 1996; Hao et al., 2017). Mean [Br⁻]/[Cl⁻] \approx 1 - 2 \times 10⁻³ in modern terrestrial waters (Edmunds, 1996; Magazinovic et al., 2004), suggesting mean [Br⁻] = 0.1 - 0.2 μ M. Mean iodide concentrations in modern terrestrial waters is reported as 40 nM (range: 0.1 nM - 0.6 μ M) (Fuge & Johnson, 1986), and it is not clear that I⁻ is generally correlated with Cl⁻ as Br⁻ seems to be (e.g.,

Worden 1996). We therefore consider both mean-I (40 nM) and high-I (0.6 μM) compositions. Estimates of $[\text{Fe}^{2+}]$ in riverine waters on early Earth span 0.1 μM - 0.1 mM (Halevy et al., 2017; Hao et al., 2017), and we consider this range. Hao et al. (2017) predict Archean river water to have $\text{pH} \leq 6.34$, for which Fe^{2+} should mainly present as Fe_{aq}^{2+} (King, 1998; Tabata et al., 2021). We take $[\text{HCO}_3^-]$ from Hao et al. (2017), and calculate $[\text{CO}_3^{2-}]$ from it. We take the bracketing range of $[\text{NO}_3^-]$ from Ranjan et al. (2019), scaled by $0.01 \times$ to remove the assumption of a high drainage ratio. We take upper bounds on $[\text{SO}_3^{2-}]$, $[\text{HSO}_3^-]$ and $[\text{HS}^-]$ from Ranjan et al. (2018) for circumneutral pH and steady-state outgassing. We consider a lower bound of 0 for all sulfur species following the assumption of Halevy (2013) for rivers.

3.3.3 Closed-Basin Carbonate Lake

Closed-basin carbonate lakes have been proposed as venues for prebiotic chemistry, because the elevated carbonate concentrations in these lakes suppresses $[\text{Ca}^{2+}]$, permitting the accumulation of phosphate to prebiotically-relevant concentrations (Toner & Catling, 2020). For a representative endmember, we consider a closed basin carbonate lake with 10^{-2} mol/kg phosphorus, corresponding to the upper edge of phosphorus concentrations in the sample of closed-basin carbonate lakes reported by Toner & Catling (2020). Cl^- and Br^- behave conservatively with P in carbonate lakes, with $[\text{Cl}^-] = 0.1 - 6$ mol/kg and $[\text{Br}^-] = 10^{-3} - 10^{-2}$ mol/kg for $[\text{P}] = 10^{-2}$ mol/kg (Toner & Catling, 2020). In projecting from Toner & Catling (2020), we simplify the calculation by approximating molarity as molality; we contend this approximation to suffice for the order-of-magnitude estimates we seek. Iodine is proposed to be delivered to surface waters via rainfall, and so we might expect it to be evaporatively concentrated in closed-basin lakes; however, we located no reports of evaporative iodide concentration in composition studies of such lakes (Fuge & Johnson, 1986; Toner & Catling, 2020; Hirst, 1995; Mochizuki et al., 2018; Eugster & Jones, 1979; Friedman et al., 1976). We therefore consider a bracketing range of $[\text{I}^-]$ equal to the freshwater lake scenario. We take $\text{Fe}_{aq}^{2+} = 0$, as high carbonate concentrations should suppress Fe_{aq}^{2+} due to siderite precipitation (Toner & Catling, 2020). Toner & Catling (2020) do not report $[\text{HCO}_3^-]$ or $[\text{CO}_3^{2-}]$ for closed-basin carbonate lakes on early Earth, but do calculate that a bracketing range of $\text{pCO}_2 = (0.01 \text{ bar}, 1 \text{ bar})$ to correspond to $\text{pH} = (9, 6.5)$ in such lakes. We convert these estimates to approximate bracketing ranges on $[\text{HCO}_3^-]$ and $[\text{CO}_3^{2-}]$ under assumption of equilibrium (Sander, 2015; Rumble, 2017). We take $[\text{NO}_3^-]$ from Ranjan et al. (2019). We consider a lower bound of 0 for all sulfur species following the assumption of Halevy (2013) for riverine waters. We take upper bounds on $[\text{HS}^-]$, $[\text{SO}_3^{2-}]$ and $[\text{HSO}_3^-]$ from Ranjan et al. (2018) for steady-state outgassing, for $\text{pH} = 7$ and $\text{pH} = 9$. The upper limits listed on $[\text{SO}_3^{2-}]$ and $[\text{HSO}_3^-]$ cannot simultaneously be achieved, because they correspond to different pHs. Our conclusions are robust to this inconsistency, because even at their respective upper limits SO_3^{2-} and HSO_3^- are not the dominant absorbers in the carbonate lake scenario.

3.3.4 Ferrous Lakes

Ferrocyanide lakes have been proposed to form when ferrocyanide salt deposits are irrigated by neutral water (Toner & Catling, 2019; Sasselov et al., 2020). Ferrocyanide is an extremely potent UV absorber, motivating us to consider transmission in such ferrocyanide lakes. Notably, ferrocyanide has been invoked in UV-dependent prebiotic chemistries, providing an opportunity to check their geochemical self-consistency (J. Xu et al., 2018; Mariani et al., 2018; Rimmer et al., 2018). We approximate the composition of a ferrocyanide lake as the freshwater lake, but with the Fe^{2+} present as $\text{Fe}(\text{CN})_6^{4-}$ instead.

4 Results

4.1 Prebiotic Ocean

The prebiotic ocean efficiently attenuated shortwave UV radiation, but may have admitted longer-wavelength UV radiation to depths of meters (Figure 1). In the low-absorption endmember, the absorption is dominated by the halides, especially Br^- at shorter wavelengths and I^- at longer wavelengths. In the high-absorption endmember scenario, absorption is dominated by Br^- at shorter wavelengths and Fe_{aq}^{2+} at longer wavelengths. Halides confine the shortest-wavelength UV photons to the surface of the ocean: in even the low-absorption endmember scenario, the ocean is optically thick¹ at ≤ 220 nm for depths $d \geq 7 \pm 1$ cm, driven primarily by Br^- . Longer-wavelength radiation may penetrate to much greater depths, with the absorbers considered here permitting penetration of the ~ 260 nm radiation responsible for nucleotide degradation to a depth of meters in even the high-absorption endmember scenario.

4.2 Prebiotic Terrestrial Waters

4.2.1 Freshwater Lakes

The transparency of shallow freshwater lakes depends strongly on the abundances of Fe^{2+} and S(IV) species (sulfite, bisulfite). In the low-absorption endmember scenario, freshwater lakes are essentially transparent in the UV, with depths of meters required for non-negligible attenuation of UV across most of the UV (Figure 2). However, in the high-absorption endmember scenario, shortwave UV is shielded due to sulfite, with secondary shielding from nitrate and Fe_{aq}^{2+} . For radiation with wavelengths ≤ 235 nm, the high-absorption endmember freshwater lake is optically thick for depths $d \geq 9.6 \pm 0.4$ cm. However, even the highly absorptive endmember remains optically thin to the $\gtrsim 260$ nm radiation which dominates nucleotide photolysis down to a depth of 1.4 ± 0.2 m.

4.2.2 Closed-Basin Carbonate Lakes

Closed-basin carbonate lakes can be more UV-opaque compared to the prebiotic ocean (Figure 3). Elevated $[\text{Br}^-]$ robustly limits absorption at short wavelengths; in even the low-absorption endmember scenario, ≤ 220 nm radiation is efficiently extinguished (i.e., is in the optically thick regime) for depths of $> 3.2 \pm 0.6$ cm. Radiation at 260 nm is robustly available for depths $\leq 1.04 \pm 0.07$ m even in the high absorption endmember scenario, but is depleted at depths of a few meters, driven by nitrate absorption with contributions from sulfite.

4.3 Ferrocyanide Lakes

Ferrocyanide lakes may have been low-UV environments (Figure 4). Ferrocyanide is a stronger, and more crucially, broader UV absorber than Fe^{2+} , able to attenuate UV across the near-UV range relevant to prebiotic chemistry. Attenuation due to ferrocyanide is minimal in the low-absorption endmember scenario. However, for the high absorption endmember, the ferrocyanide lake becomes optically thick by $d = 11 \pm 3$ cm across 200–300 nm. Photochemical derivatives of ferrocyanide, such as nitroprusside and ferricyanide, are similarly potent UV absorbers, suggesting ferrocyanide-rich lakes will remain UV-poor even if some of the ferrocyanide is photochemically processed into these forms (J. Xu et al., 2018; Mariani et al., 2018; Ross et al., 2018; Strizhakov et al., 2014). Ferrocyanide and derived compounds may therefore have been strong "sunscreens" in select lacustrine environments on early Earth, if present at elevated concentrations as postulated by some

¹ Incident flux attenuated by $\geq \frac{1}{e}$ (Thomas & Starnes, 2002)

authors and invoked by others (J. Xu et al., 2018; Toner & Catling, 2019; Sasselov et al., 2020).

5 Discussion

In Ranjan & Sasselov (2016), we argued that UV radiation down to wavelengths of ~ 204 nm would have been available for aqueous prebiotic chemistry on early Earth, motivated by the transmission of the atmosphere and of pure water. However, prebiotic waters were likely not pure. In this paper, we re-examine the conclusion of Ranjan & Sasselov (2016) by considering potential UV absorbers that might have been present in prebiotic waters.

5.1 Terrestrial Freshwater Systems May Have Been UV-Transparent

Prebiotic terrestrial freshwaters may have been largely transparent in the UV. In the low-absorption endmember scenario for terrestrial freshwater lakes, shallow lakes could have been transparent down to depths of meters across most of the >200 nm wavelength range admitted by the prebiotic atmosphere, meaning that UV radiation may have been a pervasive aspect of the surficial prebiotic milieu. Some works assume UV-opaque prebiotic pond waters, based on extrapolation of modern natural waters; however, the opacity of modern terrestrial waters in the UV is generally due to biogenic dissolved organic compounds (e.g., Morris et al. 1995; Markager & Vincent 2000; Laurion et al. 2000; Pearce et al. 2017). Indeed, even on modern Earth, waters with low biological productivity are transparent to a depth of ≥ 3 m down to the 300 nm threshold to which their transmission has been characterized (Smith & Baker, 1981; Morel et al., 2007). Prebiotic freshwaters may have been similarly transparent, unless abiotic processes were comparably efficient to modern productive ecosystems in generating organics (e.g., potentially in the immediate aftermath of a large impact; Zahnle et al. 2020).

5.2 Shortwave UV Was Likely Attenuated in Diverse Prebiotic Waters

While prebiotic natural waters in general were not necessarily opaque across the UV (200–300 nm), shortwave UV (≤ 220 nm) was attenuated in diverse prebiotic waters. Numerous prebiotic absorbers strongly attenuate shortwave UV, even if they absorb longwave UV only weakly. In particular, in high-salinity waters like the prebiotic ocean and carbonate lakes, the halide anions, especially Br^- , efficiently attenuate shortwave UV. In even the low-absorption endmembers, $\lambda \leq 220$ nm radiation is restricted to depths $d \leq 7 \pm 1$ cm in the prebiotic ocean, and $d \leq 3.2 \pm 0.6$ cm in the carbonate lake scenario (Figure 5). Shortwave UV may have been even more strongly attenuated in some waters: for example, in the high-absorption endmember for the carbonate lake scenario, nitrate absorption restricts $\lambda \leq 230$ nm UV to $d \leq 0.43 \pm 0.06$ cm. Such nitrate concentrations would only have been available in shallow closed-basin lakes with large drainage ratios, and only if atmospheric NO_x^- production rates were at the upper edge of the predicted range (Ranjan et al., 2019). Shortwave UV may have been restricted in prebiotic terrestrial waters in general, if prebiotic terrestrial sulfite concentrations were at the upper edge of what has been proposed in the literature (Figure 2). However, these literature estimates of prebiotic terrestrial sulfite concentrations consider only thermal processes and neglect photolytic loss mechanisms, meaning they be overestimates; further modelling including sulfite photolysis is required to rule on this possibility (Deister & Warneck, 1990; Fischer & Warneck, 1996; Halevy, 2013; Ranjan et al., 2018). In sum, shortwave UV may have been strongly attenuated in diverse prebiotic waters, including saline lakes and closed-basin lakes, due to the action of species like Br^- and nitrate.

5.3 Broadband UV Was Attenuated in Some Prebiotic Waters

While diverse prebiotically-plausible absorbers are capable of attenuating short-wave UV, fewer prebiotic absorbers are capable of broadband UV attenuation, including the longer-wavelength UV photons which dominate the early Sun’s UV output and hence prebiotic photoprocesses like nucleobase photolysis. One prebiotically-proposed family of broadband UV absorbers are compounds derived from ferrous iron. In particular, ferrocyanide is a strong, broad UV absorber. In the high-absorption endmember scenario for ferrocyanide lakes, ferrocyanide would have suppressed (optical depth >1) ≤ 260 nm radiation for $d \geq 1.8 \pm 0.5$ cm, and ≤ 300 nm radiation for $d \geq 11 \pm 3$ cm (Figure 6). Photochemical derivatives of ferrocyanide, such as ferricyanide and nitroprusside, are similarly effective broadband UV screens (Figure B11). Ferrocyanide lakes and their derivative waters would have been low-UV environments at depth on early Earth.

The existence and prevalence of ferrocyanide lakes on early Earth is uncertain. In particular, even if ferrocyanide lakes form as proposed by Toner & Catling (2019), ferrocyanide undergoes photoaquation under irradiation by ≤ 400 nm radiation (Ašperger, 1952). Toner & Catling (2019) argue that rapid back-reaction stabilizes ferrocyanide against this photodecomposition, based on the experimental study of Ašperger (1952). However, the measurements of Ašperger (1952) were not conducted in prebiotically-representative conditions. In particular, their UV irradiation was not representative of prebiotic UV irradiation, and the ferrocyanide concentrations used in their study were extremely high (≥ 50 mM). It is not clear whether ferrocyanide lakes would remain stable under more prebiotically-representative conditions; detailed measurements and modelling of ferrocyanide photochemistry in prebiotically-relevant conditions are required. Alternately, detection of remnants of ferrocyanide-rich environments on Mars (e.g., ferrocyanide salt deposits) might inform our understanding of the prevalence such systems on early Earth (Sasselov et al., 2020; Mojarro et al., 2021).

In addition to ferrocyanide, other ferrous iron compounds like FeSO_4 and FeCl_2 may also have acted as prebiotic “sunscreens”, thanks to their broadband UV absorption; however, much higher concentrations of these compounds are required compared to ferrocyanide due to their much lower molar absorption in the UV (Figure B11). Additionally, their formation is not thermodynamically favored relative to Fe^{2+} under conditions relevant to natural waters on modern Earth (King, 1998), and may not have been favored on early Earth either; modelling under prebiotic Earth conditions is required to definitively rule on this question. Finally, the abundance of Fe^{2+} itself in natural waters on early Earth remains debated (Konhauser et al., 2017; Halevy et al., 2017; Hao et al., 2017). Detailed, focused modelling of Fe^{2+} abundances and speciation in prebiotic waters on early Earth is required to estimate the prevalence of Fe^{2+} -derived “sunscreens” such as ferrocyanide in natural waters on early Earth

We do not recover the finding of Cleaves & Miller (1998) that Fe^{2+} in isolation would be an effective broadband sunscreen at concentrations corresponding to the prebiotic ocean. We report a molar absorbance for the Fe^{2+} ion (as $\text{Fe}(\text{BF}_4)_2$; Section B24) at 260 nm ($15 \pm 4 \text{ M}^{-1} \text{ cm}^{-1}$) that is approximately consistent with Fontana et al. (2007) and Heinrich & Seward (1990) but two orders of magnitude lower than Cleaves & Miller (1998) ($1630 \text{ M}^{-1} \text{ cm}^{-1}$). The molar absorbances of FeCl_2 , FeSO_4 , and FeOH^+ at 260 nm are also significantly below that reported by Cleaves & Miller (1998) (Anbar & Holland, 1992; Fontana et al., 2007). We speculate that one possible explanation might be formation of Fe^{2+} complexes in the study of Cleaves & Miller (1998). At slightly basic pH, characteristic of the modern ocean conditions simulated by Cleaves & Miller (1998), Fe^{2+} may have complexed with OH^- and/or CO_3^{2-} (King, 1998), and the absorption properties of such complexes may differ from Fe_{aq}^{2+} . Our findings for the prebiotic ocean are more consistent with those of Anbar & Holland (1992) for the Archaean ocean, who reported efficient attenuation of shortwave UV in the early ocean but the possibility of transmittance of longer-wavelength UV to a depth of meters.

5.4 Implications for Prebiotic Chemistry

Of the species considered in this study, we identify no ubiquitous absorber capable of attenuating broadband UV (200-300 nm) in prebiotic natural waters. Indeed, prebiotic freshwaters may have been essentially transparent in the UV. Prebiotic chemistries which are adversely affected by UV irradiation (UV-avoidant) must either be demonstrated to be so productive as to outpace UV degradation under prebiotic conditions, or invoke a UV-shielded prebiotic milieu (e.g., the organic-haze shielded aftermath of a large impact; Benner et al. 2019). UV light in the $\sim 240 - 300$ nm wavelength range was not significantly attenuated by the geologically-derived solutes considered in this study in most terrestrial prebiotic waters, meaning that low-pressure mercury lamps with primary emission at 254 nm remain reasonable proxies for UV flux in initial simulations of prebiotic chemistry. However, follow-up studies (e.g., characterization of action spectra) are required to verify that pathways discovered with such sources could have functioned in realistic natural environments on prebiotic Earth (Ranjan & Sasselov, 2016; Todd et al., 2018; Rimmer et al., 2021).

Diverse prebiotic absorbers are capable of attenuating shortwave UV (≤ 220 nm). The general prebiotic importance of removal of shortwave UV (≤ 220 nm) should not be overstated, because most of the young Sun’s UV flux was delivered at wavelengths > 220 nm (Claire et al., 2012). In particular, shallow saline waters do not shield the canonical nucleobases, nucleosides, and nucleotides, whose photolysis is expected to be dominated by the longwave (~ 260 nm) bands (Voet et al., 1963; Todd et al., 2020). Similarly, the photolysis of 2-aminothiazole and the photoconversion of cytidine to uridine are not inhibited in saline waters (Todd et al., 2019, 2020). However, the photolyses of 2-aminooxazole and 2-aminoimidazole, intermediates with proposed roles in prebiotic nucleotide synthesis and activation (Powner et al., 2009; Patel et al., 2015; Li et al., 2017), are dominated by < 230 nm radiation under early Earth conditions and their photodestruction lifetimes are hence modestly enhanced in highly saline waters. Todd et al. (2019) estimate half-lives of these molecules to photodestruction to be $\approx 7, 26,$ and 99 hours on early Earth; the half-lives of these molecules to direct photodestruction may be enhanced by up to a factor of a few in carbonate lakes by halide photoabsorption (Appendix C). Saline systems have been disfavored as venues for prebiotic chemistry, on the argument that high salt concentrations generally inhibit lipid membrane formation (e.g., Deamer & Damer 2017). However, some experimental work suggests that some amphiphile mixtures can form stable vesicles at oceanic salinity or higher, and indeed that some families of amphiphiles *require* salinity for vesicle formation (Namani & Deamer, 2008; Maurer & Nguyen, 2016; H. Xu et al., 2017; Maurer, 2017). We therefore argue that it is premature to dismiss saline waters as venues for prebiotic chemistry. Indeed, they may be favorable environments for the accumulation of molecules whose concentrations on early Earth are limited by ≤ 220 nm photolysis.

Waters rich in ferrous iron compounds such as ferrocyanide were low-UV (UV-shielded) environments. Such waters may have been favorable environments for UV-avoidant prebiotic chemistries. For example, Pearce et al. (2017) propose that meteoritically-delivered nucleobases in prebiotic ponds under the assumption that prebiotic pond-water was UV-opaque and could shield meteoritic nucleobases from photolysis. In a 1 m-deep lake with composition corresponding to the high-absorption endmember scenario for ferrocyanide lakes, the lifetimes of the nucleobases to direct photolysis would be enhanced by ~ 2 orders of magnitude, making such waters potential candidates for the meteoritic delivery scenario (Appendix C). By the same token, ferrous-rich lakes may be poor environments for UV-dependent prebiotic pathways. For example, the photoisomerization of diaminomaleonitrile (DAMN) to 5-aminoimidazole-4-carbonitrile (AICN), an intermediate for purine nucleobase synthesis, requires irradiation by $\lesssim 300$ nm photons, which could be strongly attenuated in ferrocyanide-rich lakes (Ferris & Orgel, 1966; Cleaves, 2012; Boulanger et al., 2013; Yadav et al., 2020). Similarly, the UV-driven deamination

of cytidine to form uridine, which is driven by 200-300 nm photons could be inhibited in ferrocyanide-rich waters (Powner et al., 2009; Todd et al., 2020). Solvated electron production by UV photoirradiation of the ferrocyanide-sulfite system has been proposed to efficiently drive HCN homologation, but it is unknown whether ferrocyanide and/or sulfite is the photoactive agent, and if solely the latter, whether the chemistry can function with the dilute, optically thin ferrocyanide required for sulfite photolysis (J. Xu et al., 2018; Ritson et al., 2018; Green et al., 2021). We encourage further investigation into these questions in order to better understand the prebiotic potential of this chemistry.

In our discussion so far, we have focused on the implications of absorption of UV radiation by prebiotic solutes for direct photochemical processes like excitation or photolysis of biomolecules. However, the UV energy absorbed by prebiotic absorbers must be dissipated, and while it may be dissipated thermally, it may also be dissipated through the formation of high-energy species which can participate in further chemistry. For example, the halides, sulfite/sulfide, and ferrocyanide generate solvated electrons (e_{aq}^-) and oxidized radicals upon UV irradiation, which are reactive and may trigger further chemistry (Jortner et al., 1964; Sauer et al., 2004). Such further chemistry may be destructive of biomolecules, meaning that even in waters with high concentrations of UV-absorbing compounds, UV light may indirectly suppress biomolecule accumulation. This condition must be checked by prebiotic chemistries invoking an aqueous UV "sunscreen". On the other hand, such further chemistry may also be productive. For example, Liu et al. (2021) report irradiation of SO_3^{2-} and HCO_3^- to lead to abiotic carbon fixation driven by e_{aq}^- production from SO_3^{2-} , while the simultaneous irradiation of SO_3^{2-} and ferrocyanide leads to HCN homologation (J. Xu et al., 2018). In these chemistries, the absorber effectively converts solar UV energy into chemical free energy in the form of e_{aq}^- . In sum, photochemical transformations may occur even in UV-shielded waters, triggered by photoabsorption of the very absorber which shields the UV; proposed prebiotic chemistry which invokes an aqueous-phase UV absorber must incorporate this possibility in verifying self-consistency.

5.5 Caveats & Limitations

We have not considered $FeOH^+$ as a prebiotic sunscreen. $FeOH^+$ is a strong and broad UV absorber. Crucially, its absorption at the longer UV wavelengths where the Sun emits substantially more photons means that $FeOH^+$ is projected to have played a key role in Fe^{2+} photooxidation and subsequent deposition (Braterman et al., 1983; Anbar & Holland, 1992; Tabata et al., 2021). Because of its ability to absorb longer-wavelength UV (300-450 nm), the total photoabsorption rate of $FeOH^+$ is comparable to that of Fe^{2+} at circumneutral pH, despite much lower concentrations (Nie et al., 2017). However, its absorption at longer wavelengths does not aid its potential as a sunscreen at shorter wavelengths (200-300 nm). At these wavelengths, the potential of $FeOH^+$ as a sunscreen is limited due to its low solubility at basic pH due to $Fe(OH)_2$ precipitation. This low solubility means that $[FeOH^+]$ is low, implying large depths are required for it to significantly attenuate UV (i.e., bring the optical depth to unity). The solubility product of $Fe(OH)_2$ is $K_{sp} = 4.9 \times 10^{-17}$, and $K_{eq} = 3.02 \times 10^{-10}$ for the reaction $Fe^{2+} + H_2O \rightarrow FeOH^+ + H^+$ (Braterman et al., 1983; Rumble, 2017). For $[Fe^{2+}] = 100 \mu M$, this implies $[FeOH^+] \leq 2 \mu M$, restricting the relevance of $FeOH^+$ as an aqueous sunscreen for 200-300 nm radiation to deeper waters with $d > 6$ m.

We have considered in this work only a few of the vast diversity of natural waters. Other natural waters may have different absorption properties. For example, hot springs host high concentrations of HS^- , driven by continuous supply of H_2S from below (Kaasalainen & Stefánsson, 2011). HS^- is a strong and broad absorber, and like the ferrous iron compounds attenuates the longer-wavelength UV radiation which dominates solar UV output; some hot springs could therefore have been UV-opaque. Similarly, I^- is a strong

and broad UV absorber; in waters rich in iodine, e.g. mineral springs, I^- may provide significant UV attenuation (Fuge & Johnson, 1986).

We reiterate that the estimates of UV transmittance we present here are upper bounds. The longwave absorption of HCO_3^- and CO_3^{2-} is unconstrained, and may be important in very alkaline waters. Prebiotic natural waters may have contained absorbers other than those we consider here, and if absorptive/abundant enough, these compounds may have served as sunscreens. Examples of such compounds include silicate or basaltic dust and meteoritically-delivered or atmospherically-derived organic compounds (B. Pearce, personal communication, 7/4/2019). Further work is required to determine the wavelength-dependent molar absorptivities of these alternate absorbers, and to estimate whether they could have been present in prebiotic waters at concentrations sufficient to significantly attenuate solar UV. Finally, the products of prebiotic chemistry may themselves attenuate UV (Cleaves & Miller, 1998; Todd et al., 2021). More detailed modelling of these products and their accumulation is required to rule on this possibility.

In this work, we have constructed the bracketing low- and high-absorptivity compositional endmembers for various prebiotic waters based on literature estimates. We have not attempted self-consistent geochemical modelling of these waters to estimate their composition, in part because the relevant kinetics have not been characterized under prebiotically-relevant conditions (e.g., Ranjan et al. 2018, 2019). Similarly, our work treats UV absorbers as static, and neglects further photochemical transformations triggered by their absorption of solar UV. Our work is therefore a first approximation, subject to revision by future models capable of modelling the self-consistent photochemistry and geochemistry of prebiotic natural waters.

6 Conclusions

Prebiotic freshwaters may have been essentially transparent in the UV: UV-avoidant surficial prebiotic chemistries must invoke a UV "sunscreen" agent. Shortwave (≤ 220) UV may have been attenuated in diverse prebiotic waters, with the most important absorbers being Br^- in saline waters, and potentially sulfite in shallow lakes and nitrate in shallow closed-basin lakes. Better constraints on prebiotic NO_x^- production rates and on prebiotic sulfite loss rates are required to rule on the latter possibility. Regardless, the impact of shortwave UV attenuation is modest, because most of the UV flux from the early Sun was delivered at longer, unshielded wavelengths, with the largest impact amongst the photoprocesses we considered being a modest enhancement in the lifetimes of the prebiotic intermediates 2-aminoxazole and 2-aminoimidazole to photolysis. Measurement of the wavelength-dependent rates of prebiotic processes are required to identify other processes that may be particularly promoted or inhibited in shortwave-shielded waters. The generally widespread availability of $\sim 240\text{--}300$ nm radiation means that low-pressure mercury lamps remain suitable for initial studies of prebiotic chemistry, though more realistic irradiation is required to verify the plausibility of pathways discovered under mercury lamp irradiation.

Some natural waters may have been largely opaque in the UV. In particular Fe^{2+} -derived compounds are effective broadband "sunscreens" if present at high concentrations. Ferrocyanide is an especially potent UV absorber, and ferrocyanide lake waters would have been low-UV environments which are candidate waters for UV-avoidant origin-of-life scenarios such as the meteoritic delivery hypothesis. On the other hand, such waters may be poor environments for UV-dependent reactions such as the photodeamination of cytidine to uridine. In addition to ferrocyanide, other ferrous iron compounds like $FeSO_4$ may serve as sunscreens in shallow lakes if present at proportionately higher concentrations to compensate for their lower molar absorptivities relative to ferrocyanide and to thermodynamically favor their complexation. Fe^{2+} has been suggested to be widespread on early Earth, but the abundance and speciation of Fe^{2+} compounds on early Earth

remains uncertain; we highlight detailed modelling and/or geochemical constraints on ferrous iron concentrations and speciation in prebiotic natural (especially terrestrial) waters as a priority for UV-sensitive prebiotic chemistry.

UV light can trigger photochemistry even if attenuated by an absorber, through photochemical transformations of that absorber. In particular, irradiation of a wide range of prebiotic absorbers, such as the halides, sulfite/sulfide, and ferrocyanide, is predicted to generate e_{aq}^- and oxidized radicals. The implications of this production vary by prebiotic chemistry. To be plausible, prebiotic chemistries which invoke these absorbers must self-consistently account for the chemical effects of these by-products. The rates, timescales, and concentrations relevant for various prebiotic chemical reactions may also play a role in determining the overall self-consistency of different scenarios. We encourage further investigation in these areas to better understand the necessary environments and prebiotic plausibility of various origins-of-life chemistries.

Acknowledgments

The authors are grateful to J. Cleaves, B. Pearce, J. Toner, J. Birkmann, Y. Beyad, J. Sutherland, J. Krissansen-Totton, S. Kadoya, L. Barge, and P. Rimmer for answers to questions and/or for discussions related to this paper. The authors further thank P. Rimmer and N. Green for comments on a draft of this paper, S. Kadoya for sharing the raw model outputs from Kadoya et al. (2020), and Y. Beyad for sharing the sulfite and bisulfite absorption spectra from Beyad et al. (2014). The authors thank two anonymous referees whose feedback substantially improved this paper. The authors thank the Simons Collaboration on the Origin of Life and the Harvard Origins of Life Initiative for nurturing many fruitful conversations related to this paper.

The raw data derived from the experiments, processed data reported in this paper, and scripts used to make the plots reported in this paper can be accessed on GitHub via <https://github.com/sukritranjan/dirty-water-1/>.

Author Contributions

S.R. conceived and lead study; G. L and C. L. K. performed measurements; C. L. K. synthesized data into molar decadic absorptivities and estimated errors; S. R. and A. H. performed modelling and literature data extraction for comparison; S. R., D. D. S and Z. R. T. explored prebiotic implications.

Author Disclosures

The authors are aware of no competing interests.

Funding Statements

This work was supported in part by grants from the Simons Foundation (SCOL Award# 495062 to S.R.; 3290360 to D. D. S.). Z.R.T. acknowledges support from the NASA Hubble Fellowship Program, award# HST:HF2-51471.

References

- Anbar, A. D., & Holland, H. D. (1992, July). The photochemistry of manganese and the origin of banded iron formations. *Geochimica et Cosmochimica Acta*, 56(7), 2595-2603. doi: 10.1016/0016-7037(92)90346-K
- Ašperger, S. (1952). Kinetics of the decomposition of potassium ferrocyanide in ultra-violet light. *Transactions of the Faraday Society*, 48, 617-624.

- ASTM. (2013). *Astm d1141 standard practice for the preparation of substitute ocean water* (Tech. Rep.). American Society of Testing Materials International. Retrieved from <https://www.astm.org/Standards/D1141.htm>
- Barge, L. M. (2018). Considering planetary environments in origin of life studies. *Nature communications*, *9*(1), 1–3.
- Becker, S., Feldmann, J., Wiedemann, S., Okamura, H., Schneider, C., Iwan, K., ... Carell, T. (2019). Unified prebiotically plausible synthesis of pyrimidine and purine rna ribonucleotides. *Science*, *366*(6461), 76–82.
- Becker, S., Schneider, C., Okamura, H., Crisp, A., Amatov, T., Dejmek, M., & Carell, T. (2018). Wet-dry cycles enable the parallel origin of canonical and non-canonical nucleosides by continuous synthesis. *Nature communications*, *9*(1), 1–9.
- Beckstead, A. A., Zhang, Y., de Vries, M. S., & Kohler, B. (2016). Life in the light: nucleic acid photoproperties as a legacy of chemical evolution. *Physical Chemistry Chemical Physics*, *18*(35), 24228–24238.
- Benner, S. A., Bell, E. A., Biondi, E., Brassler, R., Carell, T., Kim, H.-J., ... Trail, D. (2019). When did life likely emerge on earth in an rna-first process? *ChemSystemsChem*.
- Bevington, P. R., & Robinson, D. K. (2003). *Data reduction and error analysis*. New York: McGraw-Hill.
- Beyad, Y., Burns, R., Puxty, G., & Maeder, M. (2014). A speciation study of sulfur (iv) in aqueous solution. *Dalton Transactions*, *43*(5), 2147–2152.
- Birkmann, J., Pasel, C., Luckas, M., & Bathen, D. (2018, 12). UV spectroscopic properties of principal inorganic ionic species in natural waters. *Water Practice and Technology*, *13*(4), 879–892. Retrieved from <https://doi.org/10.2166/wpt.2018.097> doi: 10.2166/wpt.2018.097
- Bolton, J. R., Mayor-Smith, I., & Linden, K. G. (2015). Rethinking the concepts of fluence (uv dose) and fluence rate: the importance of photon-based units—a systemic review. *Photochemistry and photobiology*, *91*(6), 1252–1262.
- Bonfio, C., Valer, L., Scintilla, S., Shah, S., Evans, D. J., Jin, L., ... Mansy, S. S. (2017). Uv-light-driven prebiotic synthesis of iron–sulfur clusters. *Nature Chemistry*.
- Boulanger, E., Anoop, A., Nachtigallova, D., Thiel, W., & Barbatti, M. (2013). Photochemical steps in the prebiotic synthesis of purine precursors from hcn. *Angewandte Chemie*, *125*(31), 8158–8161.
- Braterman, P. S., Cairns-Smith, A. G., & Sloper, R. W. (1983, May). Photo-oxidation of hydrated Fe²⁺-significance for banded iron formations. *Nature*, *303*(5913), 163–164. doi: 10.1038/303163a0
- Bywater, R. P., & Conde-Frieboes, K. (2005). Did life begin on the beach? *Astrobiology*, *5*(4), 568–574.
- Channer, D. D., De Ronde, C., & Spooner, E. (1997). The cl- br- i- composition of 3.23 ga modified seawater: implications for the geological evolution of ocean halide chemistry. *Earth and Planetary Science Letters*, *150*(3–4), 325–335.
- Claire, M. W., Sheets, J., Cohen, M., Ribas, I., Meadows, V. S., & Catling, D. C. (2012, September). The Evolution of Solar Flux from 0.1 nm to 160 μm : Quantitative Estimates for Planetary Studies. *Astrophysical Journal*, *757*, 95. doi: 10.1088/0004-637X/757/1/95
- Cleaves, H. J. (2012). Prebiotic chemistry: what we know, what we don't. *Evolution: Education and Outreach*, *5*(3), 342–360.
- Cleaves, H. J. (2013). Prebiotic chemistry: geochemical context and reaction screening. *Life*, *3*(2), 331–345.
- Cleaves, H. J., & Miller, S. L. (1998, June). Oceanic Protection of Prebiotic Organic Compounds from UV Radiation. *Proceedings of the National Academy of Science*, *95*, 7260–7263. doi: 10.1073/pnas.95.13.7260

- Cockell, C. S. (2000, October). Ultraviolet Radiation and the Photobiology of Earth's Early Oceans. *Origins of Life and Evolution of the Biosphere*, *30*, 467–500.
- Cockell, C. S. (2002, January). Photobiological uncertainties in the Archaean and post-Archaean world. *International Journal of Astrobiology*, *1*, 31–38. doi: 10.1017/S1473550402001003
- Commeyras, A., Collet, H., Boiteau, L., Taillades, J., Vandenabeele-Trambouze, O., Cottet, H., ... others (2002). Prebiotic synthesis of sequential peptides on the hadean beach by a molecular engine working with nitrogen oxides as energy sources. *Polymer International*, *51*(7), 661–665.
- Corliss, J. B., Baross, J., & Hoffman, S. (1981). An hypothesis concerning the relationships between submarine hot springs and the origin of life on earth. *Oceanologica Acta, Special issue*.
- Deamer, D., & Damer, B. (2017). Can life begin on enceladus? a perspective from hydrothermal chemistry. *Astrobiology*.
- Deamer, D., & Weber, A. L. (2010). Bioenergetics and life's origins. *Cold Spring Harbor perspectives in biology*, *2*(2), a004929.
- Deister, U., & Warneck, P. (1990). Photooxidation of sulfite (so₃²⁻) in aqueous solution. *Journal of Physical Chemistry*, *94*(5), 2191–2198.
- De Ronde, C. E., deR Channer, D. M., Faure, K., Bray, C. J., & Spooner, E. T. (1997). Fluid chemistry of archaean seafloor hydrothermal vents: Implications for the composition of circa 3.2 ga seawater. *Geochimica et Cosmochimica Acta*, *61*(19), 4025–4042.
- Edmunds, W. (1996). Bromine geochemistry of british groundwaters. *Mineralogical Magazine*, *60*(399), 275–284.
- Eugster, H. P., & Jones, B. F. (1979). Behavior of major solutes during closed-basin brine evolution. *American journal of science*, *279*(6), 609–631.
- Farber, K., Dziggel, A., Meyer, F. M., Prochaska, W., Hofmann, A., & Harris, C. (2015). Fluid inclusion analysis of silicified palaeoarchaean oceanic crust—a record of archaean seawater? *Precambrian Research*, *266*, 150–164.
- Ferris, J. P., & Orgel, L. (1966). An unusual photochemical rearrangement in the synthesis of adenine from hydrogen cyanide¹. *Journal of the American Chemical Society*, *88*(5), 1074–1074.
- Fischer, M., & Warneck, P. (1996). Photodecomposition and photooxidation of hydrogen sulfite in aqueous solution. *The Journal of Physical Chemistry*, *100*(37), 15111–15117.
- Flores, J. J., Bonner, W. A., & Massey, G. A. (1977). Asymmetric photolysis of (rs)-leucine with circularly polarized ultraviolet light. *Journal of the American Chemical Society*, *99*(11), 3622–3625.
- Fontana, I., Lauria, A., & Spinolo, G. (2007). Optical absorption spectra of fe²⁺ and fe³⁺ in aqueous solutions and hydrated crystals. *physica status solidi (b)*, *244*(12), 4669–4677.
- Friedman, I., Smith, G. I., & Hardcastle, K. G. (1976). Studies of quaternary saline lakes—ii. isotopic and compositional changes during desiccation of the brines in owens lake, california, 1969–1971. *Geochimica et Cosmochimica Acta*, *40*(5), 501–511.
- Fuge, R., & Johnson, C. C. (1986). The geochemistry of iodine—a review. *Environmental geochemistry and health*, *8*(2), 31–54.
- Genda, H., Brasser, R., & Mojzsis, S. J. (2017, December). The terrestrial late veneer from core disruption of a lunar-sized impactor. *Earth and Planetary Science Letters*, *480*, 25–32. doi: 10.1016/j.epsl.2017.09.041
- Gómez, F., Aguilera, A., & Amils, R. (2007, November). Soluble ferric iron as an effective protective agent against UV radiation: Implications for early life. *Icarus*, *191*(1), 352–359. doi: 10.1016/j.icarus.2007.04.008

- Graedel, T. E., & Keene, W. (1996). The budget and cycle of earth's natural chlorine. *Pure and Applied Chemistry*, *68*(9), 1689–1697.
- Green, N. J., Xu, J., & Sutherland, J. D. (2021). Illuminating life's origins: Uv photochemistry in abiotic synthesis of biomolecules. *Journal of the American Chemical Society*.
- Guenther, E. A., Johnson, K. S., & Coale, K. H. (2001). Direct ultraviolet spectrophotometric determination of total sulfide and iodide in natural waters. *Analytical Chemistry*, *73*(14), 3481–3487.
- Halevy, I. (2013, October). Production, preservation, and biological processing of mass-independent sulfur isotope fractionation in the Archean surface environment. *Proceedings of the National Academy of Science*, *110*(44), 17644–17649. doi: 10.1073/pnas.1213148110
- Halevy, I., Alesker, M., Schuster, E. M., Popovitz-Biro, R., & Feldman, Y. (2017, January). A key role for green rust in the Precambrian oceans and the genesis of iron formations. *Nature Geoscience*, *10*, 135–139. doi: 10.1038/ngeo2878
- Halevy, I., & Bachan, A. (2017, March). The geologic history of seawater pH. *Science*, *355*, 1069–1071. doi: 10.1126/science.aal4151
- Hanley, J. J., & Koga, K. T. (2018). Halogens in terrestrial and cosmic geochemical systems: abundances, geochemical behaviors, and analytical methods. In *The role of halogens in terrestrial and extraterrestrial geochemical processes* (pp. 21–121). Springer.
- Hao, J., Sverjensky, D. A., & Hazen, R. M. (2017). A model for late archean chemical weathering and world average river water. *Earth and Planetary Science Letters*, *457*, 191–203.
- Heinrich, C. A., & Seward, T. M. (1990, August). A spectrophotometric study of aqueous iron (II) chloride complexing from 25 to 200°C. *Geochimica et Cosmochimica Acta*, *54*(8), 2207–2221. doi: 10.1016/0016-7037(90)90046-N
- Hirst, J. F. (1995). *Sedimentology, diagenesis and hydrochemistry of the saline, alkaline lakes on the cariboo plateau, interior british columbia, canada* (Unpublished master's thesis). University of Saskatchewan, Saskatoon. (Unpublished MS Thesis)
- Holm, N. G. (1992). Why are hydrothermal systems proposed as plausible environments for the origin of life? In *Marine hydrothermal systems and the origin of life* (pp. 5–14). Springer.
- IUPAC. (1997). Compendium of chemical terminology, 2nd ed. (the "gold book"). In McNaught, A. D. & Wilkinson, A. (Eds.), (2nd ed., chap. Beer–Lambert law (or Beer–Lambert–Bouguer law)). Oxford: Blackwell Scientific Publications. Retrieved from <http://goldbook.iupac.org/terms/view/B00626> doi: <https://doi.org/10.1351/goldbook.B00626>
- Johnson, K. S., & Coletti, L. J. (2002). In situ ultraviolet spectrophotometry for high resolution and long-term monitoring of nitrate, bromide and bisulfide in the ocean. *Deep Sea Research Part I: Oceanographic Research Papers*, *49*(7), 1291–1305.
- Jortner, J., Ottolenghi, M., & Stein, G. (1964). On the photochemistry of aqueous solutions of chloride, bromide, and iodide ions. *The Journal of Physical Chemistry*, *68*(2), 247–255.
- Kaasalainen, H., & Stefánsson, A. (2011, May). Sulfur speciation in natural hydrothermal waters, Iceland. *Geochimica Cosmochimica Acta*, *75*, 2777–2791. doi: 10.1016/j.gca.2011.02.036
- Kadoya, S., Krissansen-Totton, J., & Catling, D. C. (2020). Probable cold and alkaline surface environment of the hadean earth caused by impact ejecta weathering. *Geochemistry, Geophysics, Geosystems*, *21*(1), e2019GC008734.
- Kasting, J. F. (2014). Atmospheric composition of hadean–early archean earth: The importance of co. *Geological Society of America Special Papers*, *504*, 19–28.

- King, D. W. (1998). Role of carbonate speciation on the oxidation rate of Fe(II) in aquatic systems. *Environmental Science & Technology*, 32(19), 2997–3003.
- Knauth, L. P. (1998). Salinity history of the earth's early ocean. *Nature*, 395(6702), 554.
- Knauth, L. P. (2005). Temperature and salinity history of the precambrian ocean: implications for the course of microbial evolution. *Palaeogeography, Palaeoclimatology, Palaeoecology*, 219(1), 53–69.
- Konhauser, K. O., Amskold, L., Lalonde, S. V., Posth, N. R., Kappler, A., & Anbar, A. (2007). Decoupling photochemical Fe(II) oxidation from shallow-water banded iron formation. *Earth and Planetary Science Letters*, 258(1-2), 87–100.
- Konhauser, K. O., Planavsky, N. J., Hardisty, D. S., Robbins, L. J., Warchola, T. J., Haugaard, R., ... others (2017). Iron formations: A global record of neoproterozoic to palaeoproterozoic environmental history. *Earth-Science Reviews*, 172, 140–177.
- Krissansen-Totton, J., Arney, G. N., & Catling, D. C. (2018). Constraining the climate and ocean pH of the early earth with a geological carbon cycle model. *Proceedings of the National Academy of Sciences*, 201721296.
- Kröckel, L., & Schmidt, M. A. (2014). Extinction properties of ultrapure water down to deep ultraviolet wavelengths. *Optical Materials Express*, 4(9), 1932–1942.
- Laneville, M., Kameya, M., & Cleaves, H. J. (2018). Earth without life: A systems model of a global abiotic nitrogen cycle. *Astrobiology*.
- Lathe, R. (2005). Tidal chain reaction and the origin of replicating biopolymers. *International Journal of Astrobiology*, 4(1), 19–31.
- Laurion, I., Ventura, M., Catalan, J., Psenner, R., & Sommaruga, R. (2000). Attenuation of ultraviolet radiation in mountain lakes: Factors controlling the among- and within-lake variability. *Limnology and Oceanography*, 45(6), 1274–1288.
- Lerman, A., Imboden, D., & Gat, J. (Eds.). (1995). *Physics and chemistry of lakes, second edition*. Springer-Verlag.
- Li, L., Prywes, N., Tam, C. P., O'Flaherty, D. K., Lelyveld, V. S., Izgu, E. C., ... Szostak, J. W. (2017). Enhanced nonenzymatic RNA copying with 2-aminoimidazole activated nucleotides. *Journal of the American Chemical Society*, 139(5), 1810–1813.
- Li, W., Czaja, A. D., Van Kranendonk, M. J., Beard, B. L., Roden, E. E., & Johnson, C. M. (2013, November). An anoxic, Fe(II)-rich, U-poor ocean 3.46 billion years ago. *Geochimica Cosmochimica Acta*, 120, 65–79. doi: 10.1016/j.gca.2013.06.033
- Liu, Z., Wu, L.-F., Kufner, C., Sasselov, D. D., Fischer, W., & Sutherland, J. (2021). Prebiotic photoredox synthesis from carbon dioxide and sulfite. *ChemRxiv*. Retrieved from https://chemrxiv.org/articles/preprint/Prebiotic_Photoredox_Synthesis_from_Carbon_Dioxide_and_Sulfite/13692772/1 (Accepted to XXX)
- Lowe, D. R., & Byerly, G. R. (2003). Ironstone pods in the archaean barberton greenstone belt, south africa: Earth's oldest seafloor hydrothermal vents reinterpreted as quaternary subaerial springs. *Geology*, 31(10), 909–912.
- Lyons, T. W., Rogers, K., Krishnamurthy, R., Williams, L., Marchi, S., Schwieterman, E., ... Reinhard, C. (2020). Constraining prebiotic chemistry through a better understanding of earth's earliest environments. *arXiv preprint arXiv:2008.04803*.
- Mack, J., & Bolton, J. R. (1999). Photochemistry of nitrite and nitrate in aqueous solution: a review. *Journal of Photochemistry and Photobiology A: Chemistry*, 128(1-3), 1–13.
- Magazinovic, R. S., Nicholson, B. C., Mulcahy, D. E., & Davey, D. E. (2004). Bromide levels in natural waters: its relationship to levels of both chloride and total dissolved solids and the implications for water treatment. *Chemosphere*, 57(4), 329–335.

- Mancinelli, R. L., & McKay, C. P. (1988, December). The evolution of nitrogen cycling. *Origins of Life*, *18*, 311-325. doi: 10.1007/BF01808213
- Mariani, A., Russell, D. A., Javelle, T., & Sutherland, J. D. (2018). A light-releasable potentially prebiotic nucleotide activating agent. *Journal of the American Chemical Society*.
- Markager, S., & Vincent, W. F. (2000). Spectral light attenuation and the absorption of uv and blue light in natural waters. *Limnology and Oceanography*, *45*(3), 642-650.
- Martin, W., Baross, J., Kelley, D., & Russell, M. J. (2008). Hydrothermal vents and the origin of life. *Nature Reviews Microbiology*, *6*(11), 805-814.
- Marty, B., Avice, G., Bekaert, D. V., & Broadley, M. W. (2018). Salinity of the archaean oceans from analysis of fluid inclusions in quartz. *Comptes Rendus Geoscience*, *350*(4), 154-163.
- Maurer, S. (2017). The impact of salts on single chain amphiphile membranes and implications for the location of the origin of life. *Life*, *7*(4), 44.
- Maurer, S., & Nguyen, G. (2016). Prebiotic vesicle formation and the necessity of salts. *Origins of Life and Evolution of Biospheres*, *46*(2-3), 215-222.
- McCollom, T. M. (2013, May). Miller-Urey and Beyond: What Have We Learned About Prebiotic Organic Synthesis Reactions in the Past 60 Years? *Annual Review of Earth and Planetary Sciences*, *41*, 207-229. doi: 10.1146/annurev-earth-040610-133457
- Mochizuki, A., Murata, T., Hosoda, K., Dulmaa, A., Ayushsuren, C., Ganchimeg, D., ... others (2018). Distribution of trace elements and the influence of major-ion water chemistry in saline lakes. *Limnology and Oceanography*, *63*(3), 1253-1263.
- Mojarro, A., Jin, L., Szostak, J. W., Head III, J. W., & Zuber, M. T. (2021). In search of the rna world on mars. *Geobiology*, *19*(3), 307-321.
- Morel, A., Gentili, B., Claustre, H., Babin, M., Bricaud, A., Ras, J., & Tieche, F. (2007). Optical properties of the "clearest" natural waters. *Limnology and oceanography*, *52*(1), 217-229.
- Morris, D. P., Zagarese, H., Williamson, C. E., Balseiro, E. G., Hargreaves, B. R., Modenutti, B., ... Queimalinos, C. (1995). The attenuation of solar uv radiation in lakes and the role of dissolved organic carbon. *Limnology and Oceanography*, *40*(8), 1381-1391.
- Namani, T., & Deamer, D. W. (2008). Stability of model membranes in extreme environments. *Origins of Life and Evolution of Biospheres*, *38*(4), 329-341.
- Nie, N. X., Dauphas, N., & Greenwood, R. C. (2017, January). Iron and oxygen isotope fractionation during iron UV photo-oxidation: Implications for early Earth and Mars. *Earth and Planetary Science Letters*, *458*, 179-191. doi: 10.1016/j.epsl.2016.10.035
- Pace, N. R. (1991). Origin of life-facing up to the physical setting. *Cell*, *65*(4), 531-533.
- Pascal, R. (2012). Suitable energetic conditions for dynamic chemical complexity and the living state. *Journal of Systems Chemistry*, *3*(1), 1.
- Patel, B. H., Percivalle, C., Ritson, D. J., Duffy, C. D., & Sutherland, J. D. (2015, April). Common origins of RNA, protein and lipid precursors in a cyanosulfidic protometabolism. *Nature Chemistry*, *7*, 301-307. doi: 10.1038/nchem.2202
- Pearce, B. K., Pudritz, R. E., Semenov, D. A., & Henning, T. K. (2017). Origin of the rna world: The fate of nucleobases in warm little ponds. *Proceedings of the National Academy of Sciences*, *114*(43), 11327-11332.
- Perkampus, H.-H. (1992). *Uv-vis atlas of organic compounds*. VCH.
- Pestunova, O., Simonov, A., Snytnikov, V., Stoyanovsky, V., & Parmon, V. (2005). Putative mechanism of the sugar formation on prebiotic Earth initiated by UV-radiation. *Advances in Space Research*, *36*, 214-219. doi:

- 10.1016/j.asr.2005.02.049
- Pierce, S., Vianelli, A., & Cerabolini, B. (2005). From ancient genes to modern communities: the cellular stress response and the evolution of plant strategies. *Functional Ecology*, *19*(5), 763–776.
- Poulton, S. W., & Canfield, D. E. (2011). Ferruginous conditions: a dominant feature of the ocean through earth’s history. *Elements*, *7*(2), 107–112.
- Powner, M. W., Gerland, B., & Sutherland, J. D. (2009). Synthesis of activated pyrimidine ribonucleotides in prebiotically plausible conditions. *Nature*, *459*(7244), 239–242.
- Quickenden, T., & Irvin, J. (1980). The ultraviolet absorption spectrum of liquid water. *The Journal of Chemical Physics*, *72*(8), 4416–4428.
- Ranjan, S., & Sasselov, D. D. (2016, January). Influence of the UV Environment on the Synthesis of Prebiotic Molecules. *Astrobiology*, *16*, 68–88. doi: 10.1089/ast.2015.1359
- Ranjan, S., & Sasselov, D. D. (2017, March). Constraints on the Early Terrestrial Surface UV Environment Relevant to Prebiotic Chemistry. *Astrobiology*, *17*, 169–204. doi: 10.1089/ast.2016.1519
- Ranjan, S., Todd, Z. R., Rimmer, P. B., Sasselov, D. D., & Babbin, A. R. (2019). Nitrogen oxide concentrations in natural waters on early earth. *Geochemistry, Geophysics, Geosystems*, *20*(4), 2021–2039.
- Ranjan, S., Todd, Z. R., Sutherland, J. D., & Sasselov, D. D. (2018). Sulfidic anion concentrations on early earth for surficial origins-of-life chemistry. *Astrobiology*.
- Rimmer, P. B., & Shorttle, O. (2019). Origin of life’s building blocks in carbon-and nitrogen-rich surface hydrothermal vents. *Life*, *9*(1), 12.
- Rimmer, P. B., Thompson, S. J., Xu, J., Russell, D. A., Green, N. J., Ritson, D. J., ... Quéloz, D. P. (2021). Timescales for prebiotic photochemistry under realistic surface ultraviolet conditions. *Astrobiology*. Retrieved from <http://doi.org/10.1089/ast.2020.2335>
- Rimmer, P. B., Xu, J., Thompson, S. J., Gillen, E., Sutherland, J. D., & Quéloz, D. (2018). The origin of rna precursors on exoplanets. *Science advances*, *4*(8), eaar3302.
- Ritson, D. J., Battilocchio, C., Ley, S. V., & Sutherland, J. D. (2018). Mimicking the surface and prebiotic chemistry of early earth using flow chemistry. *Nature communications*, *9*(1), 1–10.
- Ross, M., Andersen, A., Fox, Z. W., Zhang, Y., Hong, K., Lee, J.-H., ... others (2018). Comprehensive experimental and computational spectroscopic study of hexacyanoferrate complexes in water: From infrared to x-ray wavelengths. *The Journal of Physical Chemistry B*, *122*(19), 5075–5086.
- Rugheimer, S., Segura, A., Kaltenegger, L., & Sasselov, D. (2015, June). UV Surface Environment of Earth-like Planets Orbiting FGKM Stars through Geological Evolution. *Astrophysical Journal*, *806*, 137. doi: 10.1088/0004-637X/806/1/137
- Rumble, J. R. (Ed.). (2017). *Crc handbook of chemistry and physics* (98th ed.). Boca Raton, FL: CRC Press.
- Sagan, C. (1973). Ultraviolet selection pressure on the earliest organisms. *Journal of Theoretical Biology*, *39*, 195–200.
- Sagan, C., & Khare, B. N. (1971, July). Long-Wavelength Ultraviolet Photoproduction of Amino Acids on the Primitive Earth. *Science*, *173*, 417–420. doi: 10.1126/science.173.3995.417
- Sander, R. (2015, April). Compilation of Henry’s law constants (version 4.0) for water as solvent. *Atmospheric Chemistry & Physics*, *15*, 4399–4981. doi: 10.5194/acp-15-4399-2015
- Sasselov, D. D., Grotzinger, J. P., & Sutherland, J. D. (2020). The origin of life as a planetary phenomenon. *Science Advances*, *6*(6), eaax3419.
- Sauer, M. C., Crowell, R. A., & Shkrob, I. A. (2004). Electron photodetachment

- from aqueous anions. 1. quantum yields for generation of hydrated electron by 193 and 248 nm laser photoexcitation of miscellaneous inorganic anions. *The Journal of Physical Chemistry A*, *108*(25), 5490–5502.
- Shirom, M., & Stein, G. (1969). The absorption spectrum of the ferrocyanide ion in aqueous solution. *Israel Journal of Chemistry*, *7*(3), 405–412.
- Sleep, N. H. (2018, September). Geological and Geochemical Constraints on the Origin and Evolution of Life. *Astrobiology*, *18*(9), 1199–1219. doi: 10.1089/ast.2017.1778
- Smith, R. C., & Baker, K. S. (1981). Optical properties of the clearest natural waters (200–800 nm). *Applied optics*, *20*(2), 177–184.
- Sojo, V., Herschy, B., Whicher, A., Camprubí, E., & Lane, N. (2016, February). The Origin of Life in Alkaline Hydrothermal Vents. *Astrobiology*, *16*, 181–197. doi: 10.1089/ast.2015.1406
- Strizhakov, R., Tretyakov, E., Medvedeva, A., Novokshonov, V., Vasiliev, V., Ovcharenko, V., ... Bagryanskaya, E. (2014). Permethy- β -cyclodextrin spin-labeled with nitronyl nitroxide: synthesis and epr study. *Applied Magnetic Resonance*, *45*(10), 1087–1098.
- Tabata, H., Sekine, Y., Kanzaki, Y., & Sugita, S. (2021, April). An experimental study of photo-oxidation of Fe(II): Implications for the formation of Fe(III) (hydro)oxides on early Mars and Earth. *Geochimica et Cosmochimica Acta*, *299*, 35–51. doi: 10.1016/j.gca.2021.02.006
- Thomas, G. E., & Stammes, K. (2002). *Radiative transfer in the atmosphere and ocean*. Cambridge University Press.
- Todd, Z. R., Fahrenbach, A. C., Magnani, C. J., Ranjan, S., Björkbom, A., Szostak, J. W., & Sasselov, D. D. (2018). Solvated-electron production using cyanocuprates is compatible with the uv-environment on a hadean–archaeon earth. *Chemical Communications*.
- Todd, Z. R., Fahrenbach, A. C., Ranjan, S., Magnani, C. J., Szostak, J. W., & Sasselov, D. D. (2020). Ultraviolet-driven deamination of cytidine ribonucleotides under planetary conditions. *Astrobiology*.
- Todd, Z. R., Szabla, R., Szostak, J. W., & Sasselov, D. D. (2019). Uv photostability of three 2-aminoazoles with key roles in prebiotic chemistry on the early earth. *Chemical Communications*, *55*(70), 10388–10391.
- Todd, Z. R., Szostak, J. W., & Sasselov, D. D. (2021, February). Shielding from UV Photodamage: Implications for Surficial Origins of Life Chemistry on the Early Earth. *ACS Earth and Space Chemistry*, *5*(2), 239–246. doi: 10.1021/acsearthspacechem.0c00270
- Toner, J. D., & Catling, D. C. (2019). Alkaline lake settings for concentrated prebiotic cyanide and the origin of life. *Geochimica et Cosmochimica Acta*, *260*, 124–132.
- Toner, J. D., & Catling, D. C. (2020). A carbonate-rich lake solution to the phosphate problem of the origin of life. *Proceedings of the National Academy of Sciences*, *117*(2), 883–888.
- Voet, D., Gratzner, W., Cox, R., & Doty, P. (1963). Absorption spectra of nucleotides, polynucleotides, and nucleic acids in the far ultraviolet. *Biopolymers*, *1*(3), 193–208.
- Walker, J. C., & Brimblecombe, P. (1985). Iron and sulfur in the pre-biologic ocean. *Precambrian Research*, *28*(3–4), 205–222.
- Wong, M. L., Charnay, B. D., Gao, P., Yung, Y. L., & Russell, M. J. (2017, October). Nitrogen Oxides in Early Earth’s Atmosphere as Electron Acceptors for Life’s Emergence. *Astrobiology*, *17*, 975–983. doi: 10.1089/ast.2016.1473
- Worden, R. H. (1996). Controls on halogen concentrations in sedimentary formation waters. *Mineralogical Magazine*, *60*(399), 259–274.
- Xu, H., Du, N., Song, Y., Song, S., & Hou, W. (2017). Vesicles of 2-keto-octanoic

- acid in water. *Soft Matter*, *13*(11), 2246–2252.
- Xu, J., Chmela, V., Green, N. J., Russell, D. A., Janicki, M. J., Góra, R. W., . . . Sutherland, J. D. (2020). Selective prebiotic formation of rna pyrimidine and dna purine nucleosides. *Nature*, *582*(7810), 60–66.
- Xu, J., Ritson, D. J., Ranjan, S., Todd, Z. R., Sasselov, D. D., & Sutherland, J. D. (2018). Photochemical reductive homologation of hydrogen cyanide using sulfite and ferrocyanide. *Chemical Communications*.
- Yadav, M., Kumar, R., & Krishnamurthy, R. (2020). Chemistry of abiotic nucleotide synthesis. *Chemical reviews*, *120*(11), 4766–4805.
- Zafiriou, O. C. (1974). Sources and reactions of oh and daughter radicals in seawater. *Journal of Geophysical Research*, *79*(30), 4491–4497.
- Zahnle, K. J., Lupu, R., Catling, D. C., & Wogan, N. (2020, June). Creation and Evolution of Impact-generated Reduced Atmospheres of Early Earth. *The Planetary Science Journal*, *1*(1), 11. doi: 10.3847/PSJ/ab7e2c

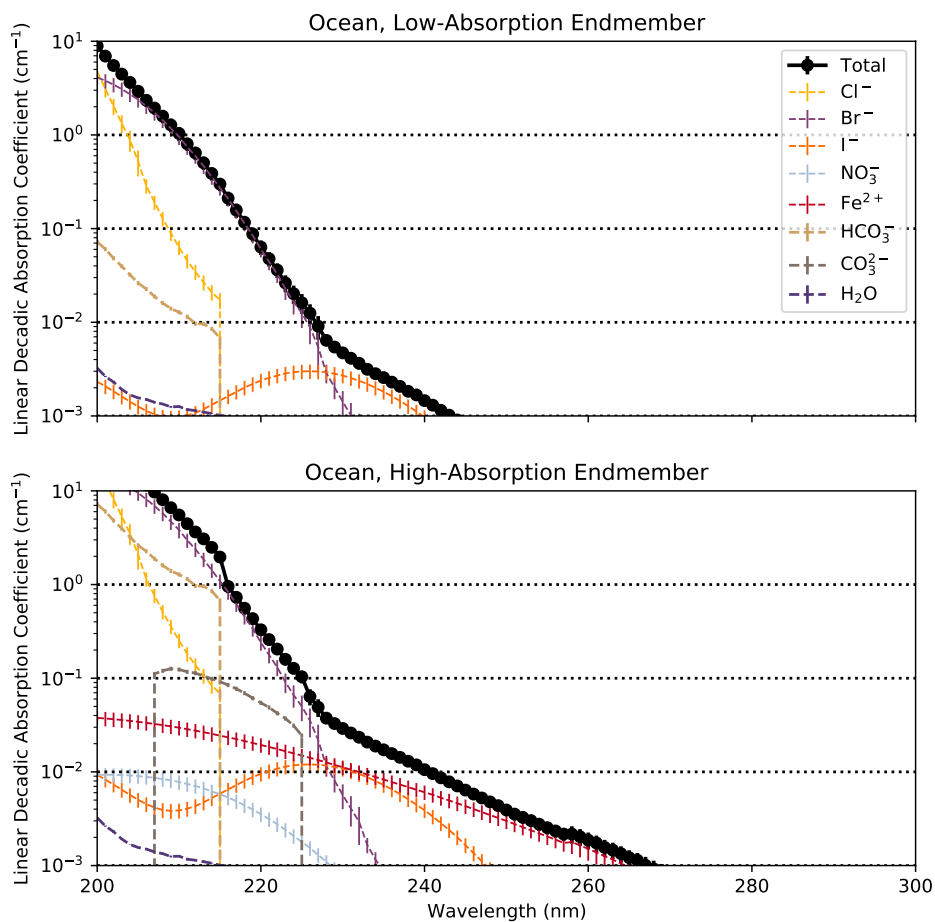


Figure 1. Simulated linear decadic absorption coefficients of the prebiotic ocean and its component solutes, for low-absorption and high-absorption endmember cases. Not all solutes are visible in each case, because the linear decadic absorption coefficients of some solutes fall below the lower limit of the y-axis across the wavelength space plotted here. The shortest-wavelength photons are extinguished in the surface layers of the ocean, but the ~ 260 nm radiation responsible for nucleotide degradation can penetrate to a depth of meters.

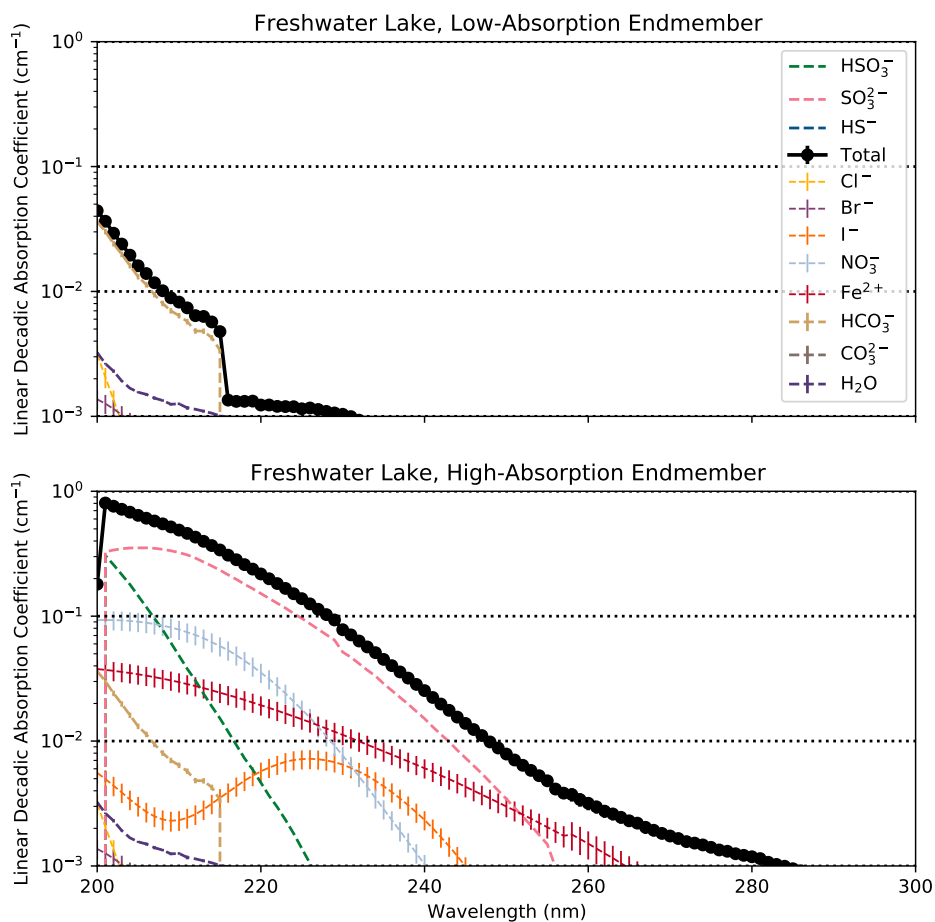


Figure 2. Simulated linear decadic absorption coefficients of the prebiotic freshwater lake and its component solutes, for low-absorption and high-absorption endmember cases. Not all solutes are visible in each case, because the linear decadic absorption coefficients of some solutes fall below the lower limit of the y-axis across the wavelength space plotted here. The freshwater lake may have been largely transparent to UV, and even in the high-absorption endmember would have been largely transparent to UV at the longer wavelengths (~ 260 nm) relevant to nucleotide photolysis.

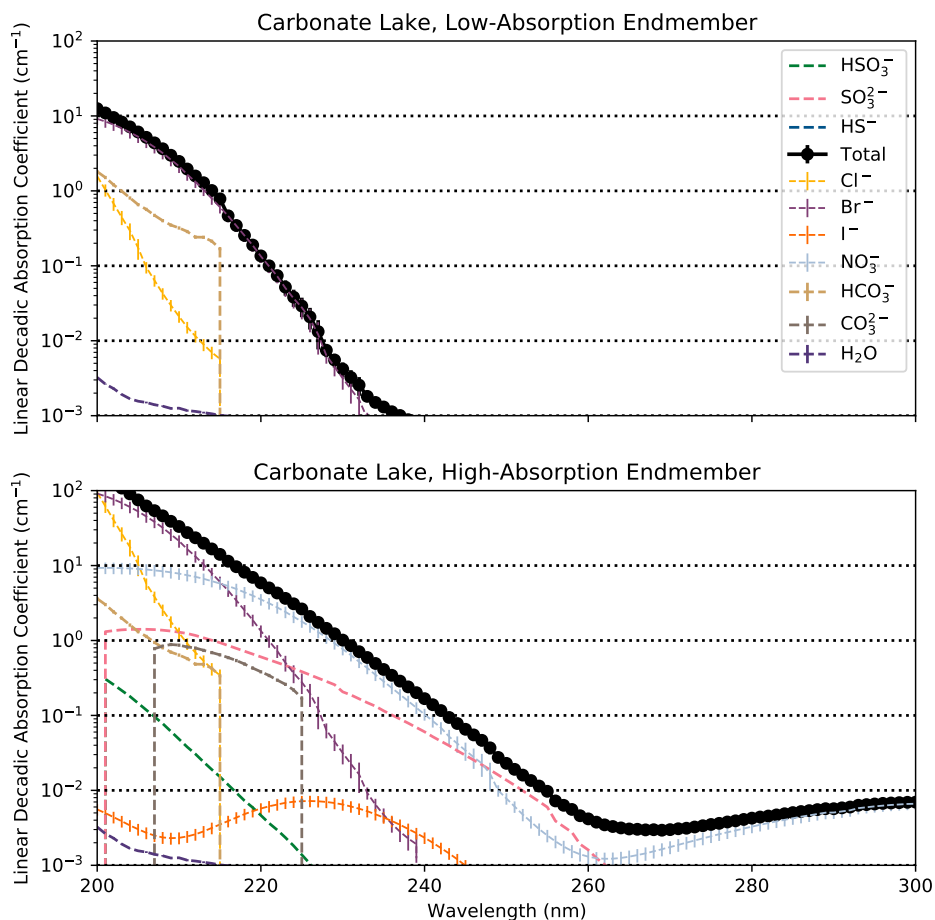


Figure 3. Simulated linear decadic absorption coefficients of the prebiotic carbonate lake and its component solutes, for low-absorption and high-absorption endmember scenario. Not all solutes are visible in each case, because the linear decadic absorption coefficients of some solutes fall below the lower limit of the y-axis across the wavelength space plotted here. The carbonate lake robustly extinguishes shortwave UV in even the low-absorption endmember scenario, driven by Br^- . In the high-absorption endmember case, longer wavelength UV would have been available throughout shallow lakes ($d < 1\text{m}$), but would have been extinguished at depths of a few meters.

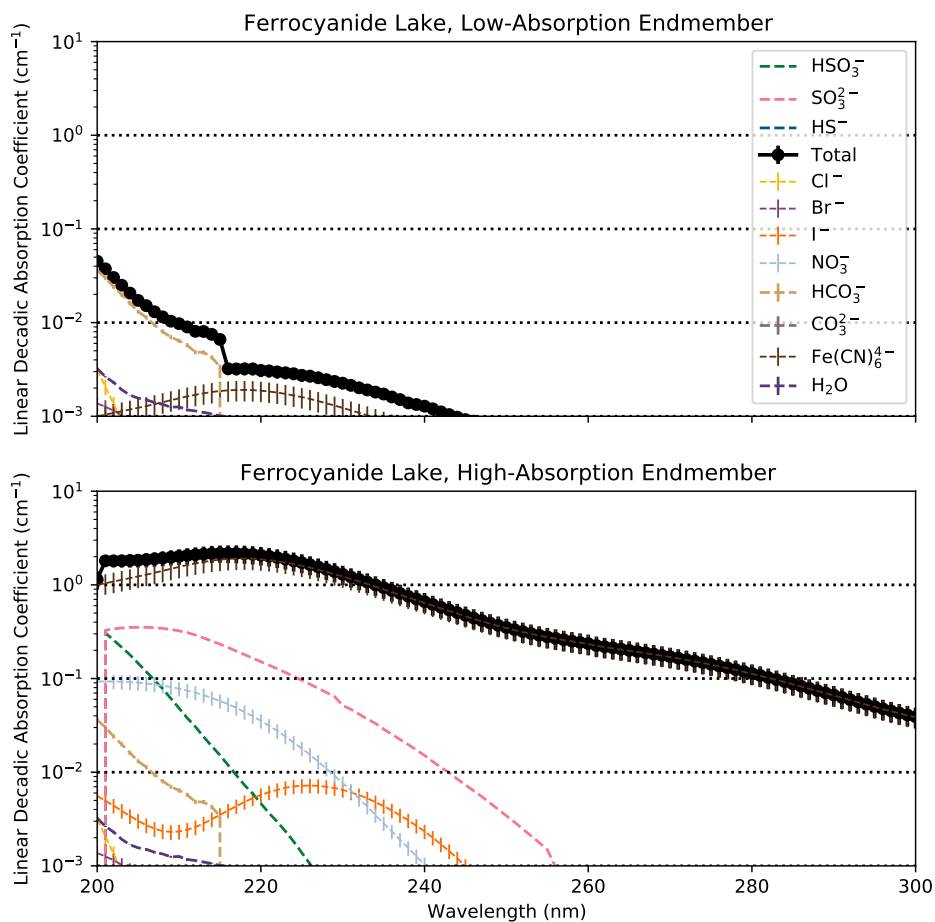


Figure 4. Simulated linear decadic absorption coefficients of the prebiotic ferrocyanide lake and its component solutes, for low-absorption and high-absorption endmember scenarios. Not all solutes are visible in each case, because the linear decadic absorption coefficients of some solutes fall below the lower limit of the y-axis across the wavelength space plotted here. Ferrocyanide is an effective sunscreen, and lakes hosting more than dilute ferrocyanide ($\gtrsim 100 \mu\text{M}$) would have been low-UV environments.

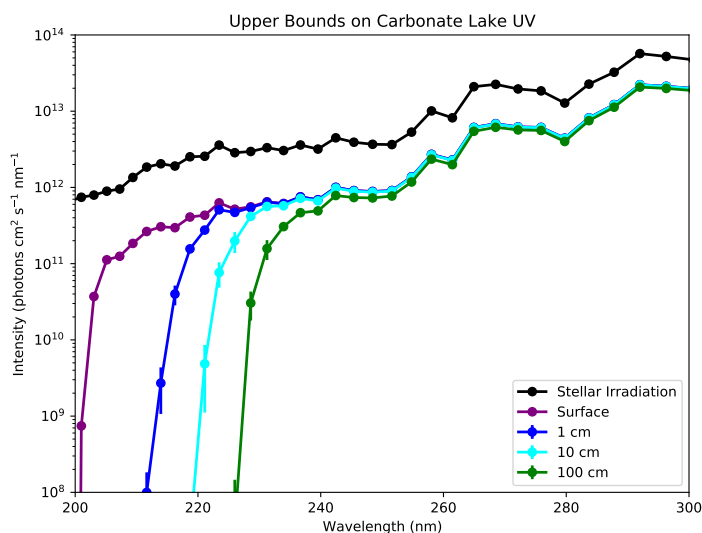


Figure 5. Estimate of actinic UV flux as a function of depth in the low-absorption endmember of the carbonate lake scenario, calculated by attenuating the surface actinic flux of Ranjan & Sasselov (2017) (their "surface radiance") by Beer-Lambert law, assuming a slant angle of 60° , atmospheric composition from Rugheimer et al. (2015), and stellar irradiation of 3.9 Ga Sun from Claire et al. (2012). In even the low-absorption endmember, attenuation of < 220 nm irradiation is significant.

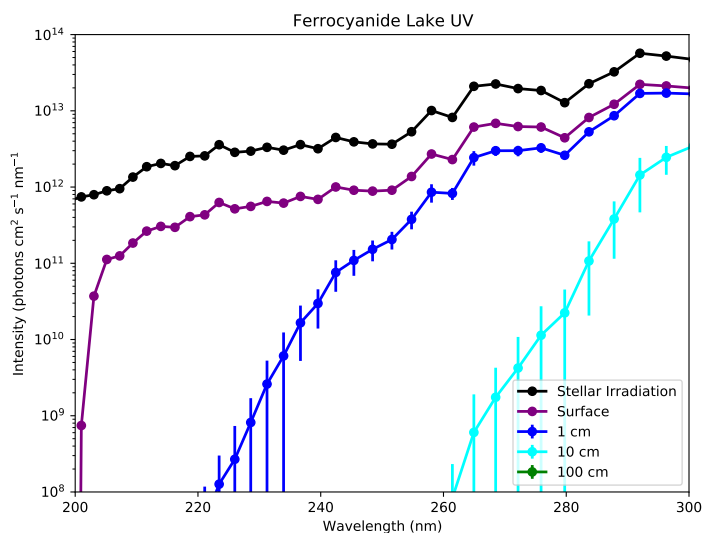


Figure 6. Estimate of actinic UV flux as a function of depth in the high-absorption endmember of the ferrocyanide lake scenario, calculated by attenuating the surface actinic flux of Ranjan & Sasselov (2017) (their "surface radiance") by Beer-Lambert law, assuming a slant angle of 60° , atmospheric composition from Rugheimer et al. (2015), and stellar irradiation of 3.9 Ga Sun from Claire et al. (2012). In the high-absorption endmember, broadband UV is extinguished at shallow depths.

Appendix A Optical Properties of Pure Water

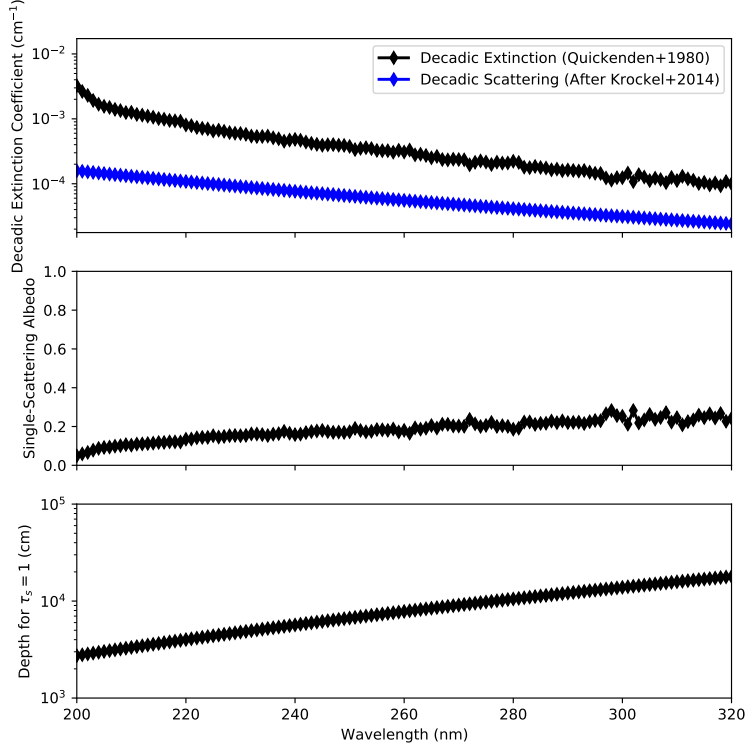


Figure A1. Decadic extinction and scattering coefficients, single scattering albedo, and the depth at which the scattering optical depth ≥ 1 as a function of wavelength for pure liquid water under standard conditions. The decadic extinction is taken from Quickenden & Irvin (1980), which remains state-of-the-art in this wavelength range (Kröckel & Schmidt, 2014). The Rayleigh scattering is calculated following Kröckel & Schmidt (2014), with the modifications that the index of refraction, n , and the pressure derivative of n at constant temperature T , $(\frac{\partial n}{\partial p})_T$, are taken to be constant at $n = 1.39$ and $(\frac{\partial n}{\partial p})_T = 0.095 \mu\text{m}^2 \text{ kN}^{-1}$.

Appendix B Molar Decadic Absorption Coefficients

B1 Measured Molar Decadic Absorption Coefficients

B11 Samples

All salts were purchased from Sigma-Aldrich (USA) at the highest available purity grade ($\geq 95\%$) and used without further purification. All samples were dissolved in LC-MS grade freshwater (LiChrosolv, Millipore Sigma, USA).

B12 Setup

The pH was measured by a pH electrode (Hach SensION + PH3, USA). The dissolved samples were kept in sealable spectrosil quartz cuvettes (9B-Q-10-GL14-C, Starna Cell's, USA) with a sample depth of 10 mm. The concentrations of the samples were kept

$\leq 0.1 \times$ the saturation concentration. Additionally the absorbance was kept between optical depth (OD) 0.005 and OD 1.1 throughout the spectral range of 200 nm to 360 nm by several dilution steps of the samples. All absorbance spectra were recorded in triplicates at 23°C by a Shimadzu UV-1900 UV-VIS spectrophotometer relative to a blank water sample, and measurements were conducted at ambient conditions unless otherwise specified.

B13 Data evaluation

After an initial solvent correction the triplicate spectra were averaged and cropped to an absorbance range between OD 0.005 and OD 1.1. The molar decadic absorption coefficients were calculated from the absorption spectra by division by the respective sample concentrations. Spectral ranges with systematic deviations, e. g. due to cuvette contamination, were excluded from the dataset. The systematic error of the spectrophotometric measurements was estimated conservatively to be about 15%. Additionally, the following errors were included in the estimate: 6% for the pipetting process, 4% for the sample masses (14% for NaS) and 5% for sample impurities. In case of pH sensitive samples, an error of up to 4% was included to account for the chemical equilibrium at the respective pH according to the Henderson-Hasselbalch equation. The statistical error for each sample was estimated from the averaging process. Table B1 gives the dilution sequence used to compile the molar absorptivity measurements.

Table B1. Measurement sequences used to determine molar decadic absorption coefficients. We report pH for the $\text{Fe}(\text{BF}_4)_2$ and $\text{K}_4[\text{Fe}(\text{CN})_6]$ measurement sequences to verify their speciation (Section B14). FeSO_4 , FeCl_2 , and $\text{Na}_2\text{Fe}(\text{CN})_5\text{NO}$ are not listed here because molar decadic absorption coefficients for those species were drawn from the literature.

Sample	Measurement Sequence
NaBr	80 μM , 400 μM , 860 μM , 2 mM, 20 mM, 100 mM
KBr	70 μM , 350 μM , 1 mM, 20 mM, 100 mM
NaCl	50 mM, 559 mM
NaI	50 μM , 100 μM , 2 mM, 50 mM, 100 mM
KI	100 μM , 2 mM, 100 mM
$\text{Fe}(\text{BF}_4)_2$	1 mM (pH=3.4), 2 mM (pH=3.2), 20 mM (pH=2.6), 50 mM (pH=2.3), 200 mM (pH=1.7)
$\text{K}_4[\text{Fe}(\text{CN})_6]$	44 μM (pH=6.5), 87 μM (pH=6.4), 174 μM (pH=6.4), 436 μM (pH=6.0)

B14 Experimental Concerns & Mitigations

We conducted our measurements at ambient conditions, i.e. in oxic air. Under oxic conditions ferrous iron slowly oxidizes. To mitigate this effect, each measurement sequences involving ferrous iron species were completed in ≤ 1 hour. We performed control experiments for the ferrous iron species under reduced oxygen conditions. We did not observe differences in the absorption spectra within the duration of our experiments, and in both cases found good agreement with the literature, suggesting that this procedure did not impact the accuracy of our approach.

Special care was taken during the cuvette cleaning process to avoid contamination. In particular, the cuvettes were cleaned solely with water; we did not clean with acetone

as we discovered in preliminary experiments that absorptivity due to residual acetone contaminated the measurements.

Fe^{2+} can complex with OH^- in basic solution (King, 1998). We therefore tracked the pH of the $\text{Fe}(\text{BF}_4)_2$ solutions to ensure they remained at the acid pH at which Fe_{aq}^{2+} is the dominant form. Conversely, in acidic solution $\text{Fe}(\text{CN})_6^{4-}$ can protonate. We tracked the pH of the ferrocyanide solutions to ensure they well exceeded $\text{pH} = 4.2$, corresponding to the pK_a of the first protonation of $\text{Fe}(\text{CN})_6^{4-}$ (Shirom & Stein, 1969).

B2 Measured Spectra of Prebiotically-Relevant Compounds & Comparison to Literature Data

In this section, we compare our measured spectra to those extracted from the literature. The literature data typically do not include uncertainty estimates. However, Birkmann et al. (2018) note that in previous studies, the uncertainty on their measurements of molar absorption coefficients was 5%, as determined by reproduction. We assume this uncertainty estimate of 5% to apply to the measurements reported in Birkmann et al. (2018) as well.

B21 Bromide (Br^-)

Figure B1 presents the molar absorption coefficients of NaBr and KBr derived from our measurements. The absorption of these species is identical to the precision of our measurements, confirming the findings of past work which indicate the anion dominates the absorption (Birkmann et al. 2018 and sources therein). Our data agree with the measurements of Birkmann et al. (2018) from 200-225 nm, and extend the spectral coverage to 240 nm. We follow Birkmann et al. (2018) in disagreeing with Johnson & Coletti (2002) at short (< 204 nm) wavelengths.

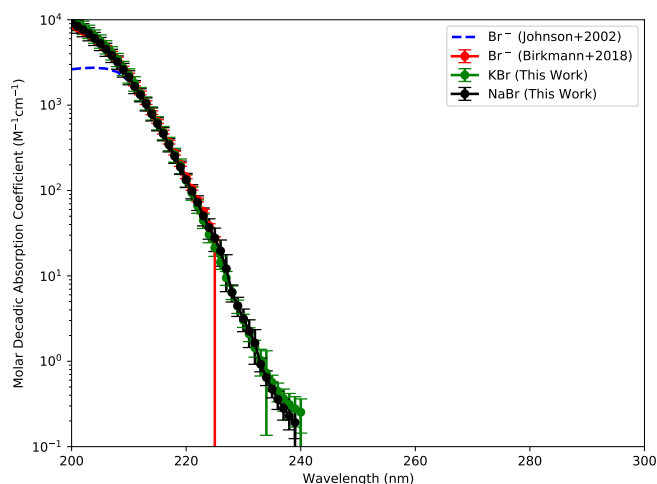


Figure B1. Molar absorption coefficients of Br^- derived from our measurements, compared to literature reports from Birkmann et al. (2018) and Johnson & Coletti (2002). Our data extend spectral coverage of Br^- absorption from 225 to 240 nm. We do not detect Br^- absorption at >240 nm.

B22 Chloride (Cl^-)

Figure B2 presents the molar absorption coefficients for NaCl derived from our measurements. We take the absorption of NaCl to be representative of Cl^- generally, based on past work (Birkmann et al., 2018), and on our own measurements of KCl absorption. Our measurements agree with Birkmann et al. (2018) from 200-215 nm, and indicate that absorption of Cl^- is much lower than reported by Perkampus (1992).

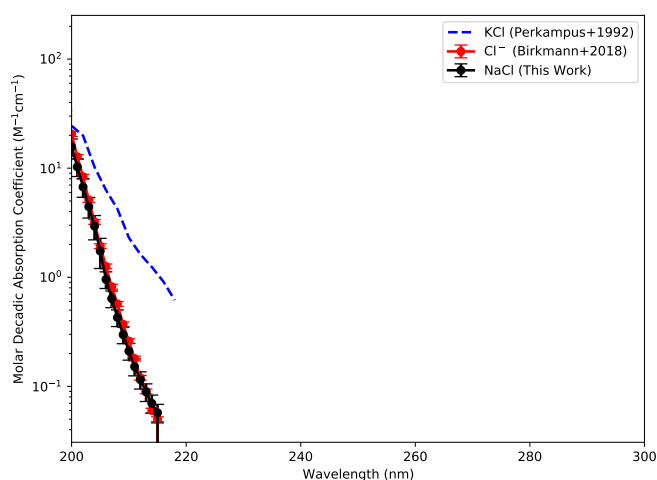


Figure B2. Molar absorption coefficients of Cl^- derived from our measurements, compared to literature reports from Birkmann et al. (2018) and Perkampus (1992). We do not detect Cl^- absorption at >215 nm.

B23 Iodide (I^-)

Figure B3 presents the molar absorption coefficients of NaI and KI derived from our measurements. Where our data for these molecules overlap in spectral coverage, they are identical to within experimental uncertainty, consistent with past reports that the anion dominates UV absorption (Birkmann et al., 2018). We therefore combine the NaI and KI molar absorptivity measurements to synthesized a generalized I^- absorption spectrum, which extend the longwave limit of spectral coverage of I^- absorption from 252 nm to 280 nm. Our measurements agree with Birkmann et al. (2018) from 200-252 nm. Our measurements generally agree with Guenther et al. (2001), but disagree slightly at their longest wavelengths of measurement.

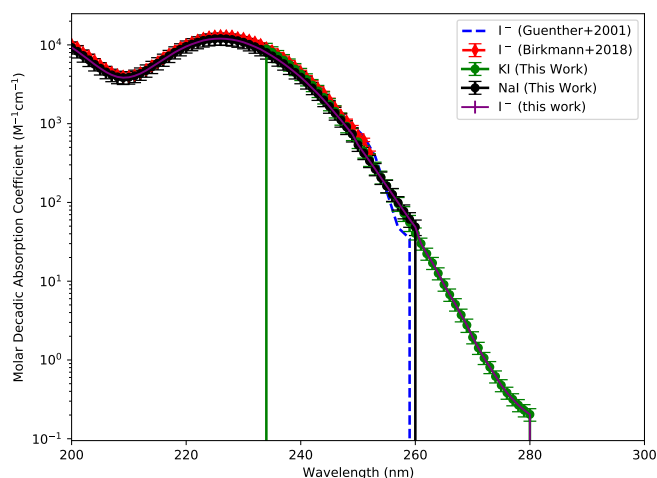


Figure B3. Measured molar absorption coefficients of I^- , compared to literature reports from Birkmann et al. (2018) and Guenther et al. (2001). Our data extend spectral coverage of I^- absorption to 280 nm. We do not detect I^- absorption at >280 nm.

B24 Fe^{2+} , as $\text{Fe}(\text{BF}_4)_2$

We represent the absorption of Fe_{aq}^{2+} by the absorption spectrum of $\text{Fe}(\text{BF}_4)_2$. Other workers (e.g., Tabata et al. 2021) instead take the absorption spectrum of Fe_{aq}^{2+} from that reported by Heinrich & Seward (1990). Heinrich & Seward (1990) derive their Fe^{2+} by reducing iron metal (Fe^0) with HCl. This means that Cl^- is present as a counter-ion in this solution, which influences the complexation and hence the UV spectrum of Fe^{2+} . Most significantly, use of Cl^- as a counter-ion leads to higher longwave UV absorption, and lower shortwave absorption Fontana et al. (2007). Comparing the UV molar absorption coefficients of solutions of FeCl_2 , FeSO_4 , $\text{Fe}(\text{NH}_4\text{SO}_4)_2$, and $\text{Fe}(\text{BF}_4)_2$, Fontana et al. (2007) report solutions of $\text{Fe}(\text{BF}_4)_2$ to have the fewest bands attributable to complexes other than the $\text{Fe}(\text{H}_2\text{O})_6^{2+}$ expected to form from Fe_{aq}^{2+} in isolation. We therefore follow Fontana et al. (2007) in not using the absorption spectrum of FeCl_2 solution to represent the absorption spectrum of Fe_{aq}^{2+} in isolation, and instead use $\text{Fe}(\text{BF}_4)_2$. In natural waters anions may in truth be present, which could enhance the absorptivity of the ferrous iron by complexation; the absorption of Fe^{2+} therefore constitutes a lower bound on the UV absorption of ferrous compounds.

Our measurement of the $\text{Fe}(\text{BF}_4)_2$ molar absorption coefficients in the UV is given in Figure B4. Our measurements generally agree with those extracted from Fontana et al. (2007), but are slightly lower than theirs from 240-280 nm. Our measurements may therefore slightly underestimate UV absorption in this range. Our conclusions, which are at the order-of-magnitude level, are robust to this possibility.

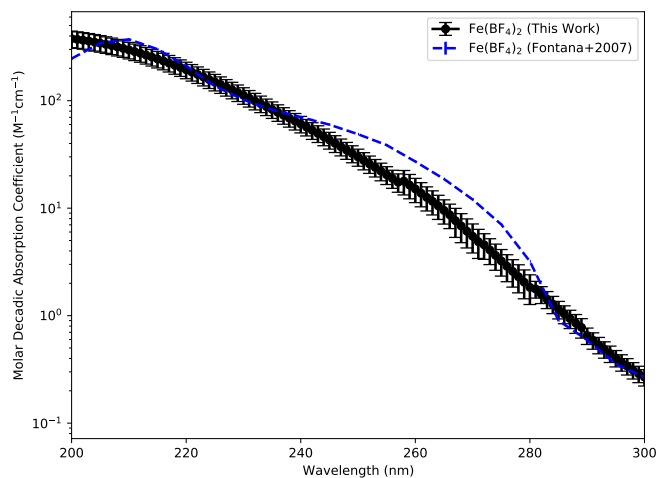


Figure B4. Measured molar absorption coefficients of $\text{Fe}(\text{BF}_4)_2$, taken as representative of ferrous iron generally, compared to literature reports from Fontana et al. (2007).

B25 Ferrocyanide

Figure B5 presents the molar absorption coefficients for $\text{K}_4\text{Fe}(\text{CN})_6$ (ferrocyanide) derived from our measurements. The molar absorption coefficients we report agree with those extracted from Ross et al. (2018), but we extend the spectral coverage blueward to 200 nm.

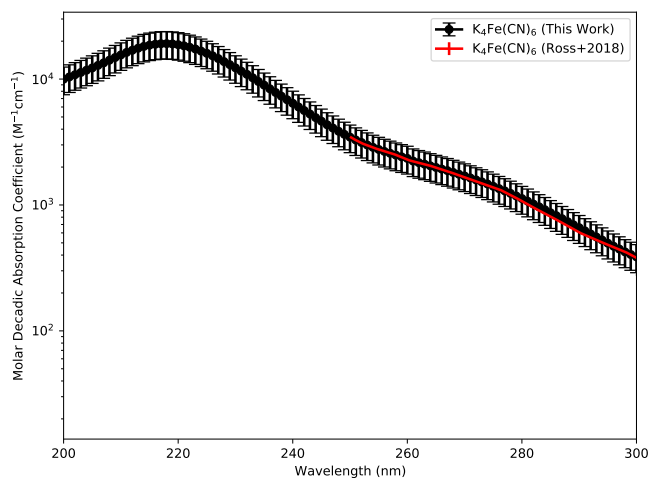


Figure B5. Measured molar absorption coefficients of $\text{K}_4\text{Fe}(\text{CN})_6$, taken as representative of ferrocyanide, compared to literature reports from Ross et al. (2018). Our data extend spectral coverage of $\text{K}_4\text{Fe}(\text{CN})_6$ absorption down to 200 nm.

B26 Nitrate

Figure B6 presents the molar absorption coefficients for NaNO_3 (nitrate) derived from our measurements. The molar absorption coefficients we report are in reasonable agreement to those we extract from Mack & Bolton (1999) and Birkmann et al. (2018).

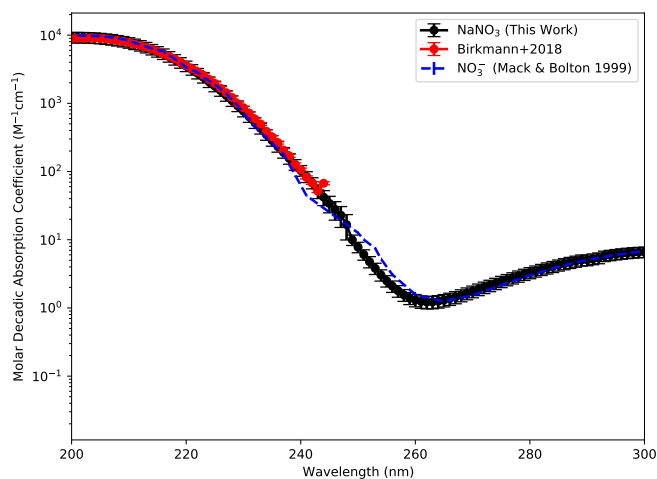


Figure B6. Measured molar absorption coefficients of NaNO_3 , taken as representative of the NO_3^- ion, compared to the literature absorption spectrum of NO_3^- of Mack & Bolton (1999) and Birkmann et al. (2018). Our measurements agree well with the literature sources.

B3 Literature-Derived Molar Decadic Absorption Coefficients

In this section, we show the molar decadic absorption coefficients we extracted from the literature. The literature data typically do not include uncertainty estimates. As in Section B2, we assume an error of 5% on the measurements reported by Birkmann et al. (2018). We propagate this uncertainty under the assumption of uncorrelated, normally-distributed error, as with our own uncertainty estimates.

B31 Sulfite

We combined the measurements of Beyad et al. (2014) and Fischer & Warneck (1996) to obtain an absorption spectrum for SO_3^{2-} . Specifically, we used the entire dataset of Beyad et al. (2014), and concatenated the molar absorptivities of Fischer & Warneck (1996) at shorter wavelengths where data from Beyad et al. (2014) was unavailable (Figure B7).

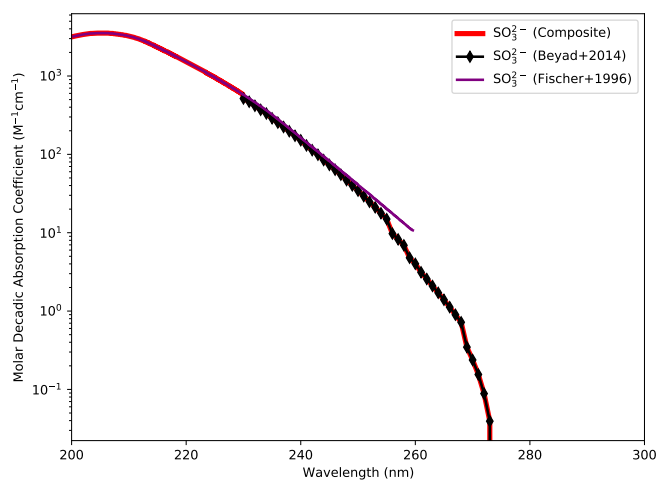


Figure B7. Molar absorption coefficients of SO_3^{2-} , derived from Beyad et al. (2014) and Fischer & Warneck (1996).

B32 Bisulfite

We combined the measurements of Beyad et al. (2014) and Fischer & Warneck (1996) to obtain an absorption spectrum for HSO_3^- . Specifically, we used the entire dataset of Beyad et al. (2014), and concatenated the molar absorptivities of Fischer & Warneck (1996) at shorter wavelengths where data from Beyad et al. (2014) was unavailable. We used a log-linear extrapolation to connect the two datasets. (Figure B7).

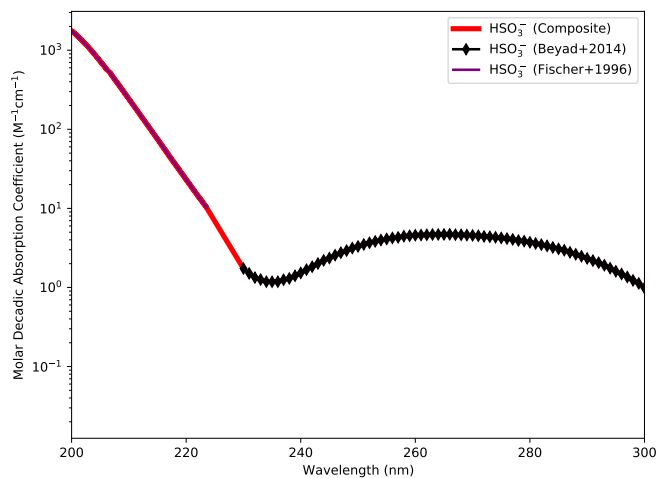


Figure B8. Molar absorption coefficients of HSO_3^- , derived from Beyad et al. (2014) and Fischer & Warneck (1996).

B4 Bisulfide

We derived molar absorption coefficients for HS^- in the UV from the absorbance spectra of $50 \mu\text{m}$ HS^- reported by Guenther et al. (2001) (Figure B9). These data terminate at 260 nm, and our experimental procedure was inadequate to reliably constrain molar absorptions at longer wavelengths. We therefore caution that HS^- may have additional absorption at longer wavelengths than we consider.

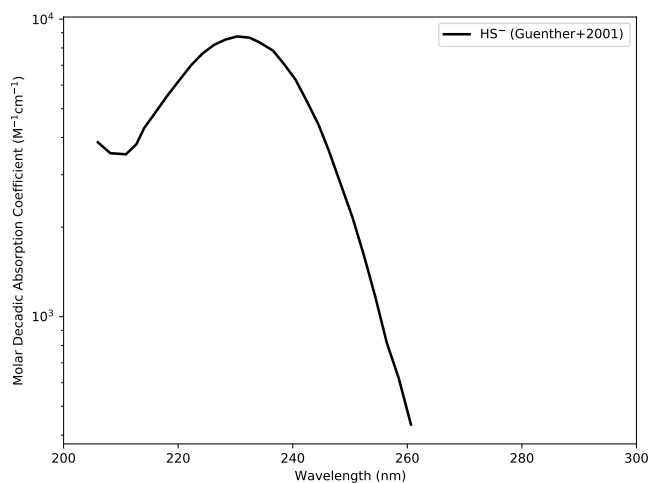


Figure B9. Molar absorption coefficients of SO_3^{2-} , extracted from Guenther et al. (2001).

B41 Carbonate and Bicarbonate

We draw molar absorption coefficients for carbonate (CO_3^-) and bicarbonate (HCO_3^-) from Birkmann et al. (2018) (Figure B10). These measured spectra terminate abruptly at relatively short wavelengths. We are not aware of constraints on the absorption of bicarbonate and carbonate at longer wavelengths, and our efforts to reliably constrain absorption at these longer wavelengths were unsuccessful. We therefore caution that carbonate and bicarbonate may have additional absorption at longer wavelengths than we consider.

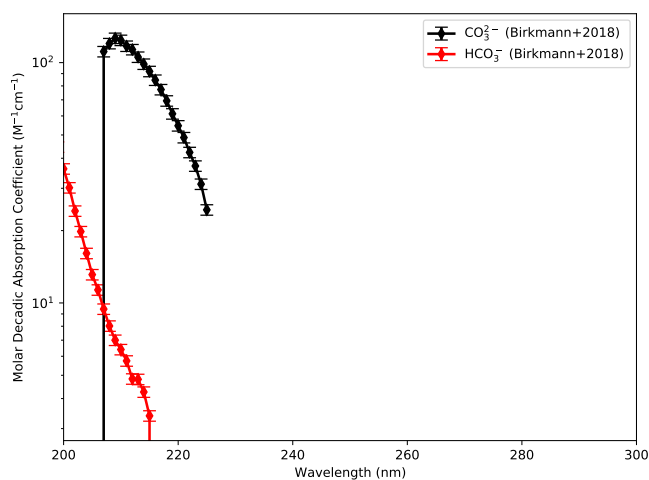


Figure B10. Molar absorption coefficients of CO_3^{2-} and HCO_3^- , from Birkmann et al. (2018).

B42 Other Fe^{2+} -Derived Compounds

FeCl_2 and FeSO_4 are potential complexes of Fe^{2+} in natural waters, and nitroprusside and ferricyanide are potential photochemical derivatives of ferrocyanide. We extract molar absorption coefficients of FeCl_2 , FeSO_4 , $\text{Na}_2\text{Fe}(\text{CN})_5\text{NO}$ (nitroprusside), and $\text{Fe}(\text{CN})_6^{3-}$ (ferricyanide) from the literature (Fontana et al., 2007; Strizhakov et al., 2014; Ross et al., 2018). Iron and cyanide are extremely absorptive in the UV (Figure B11).

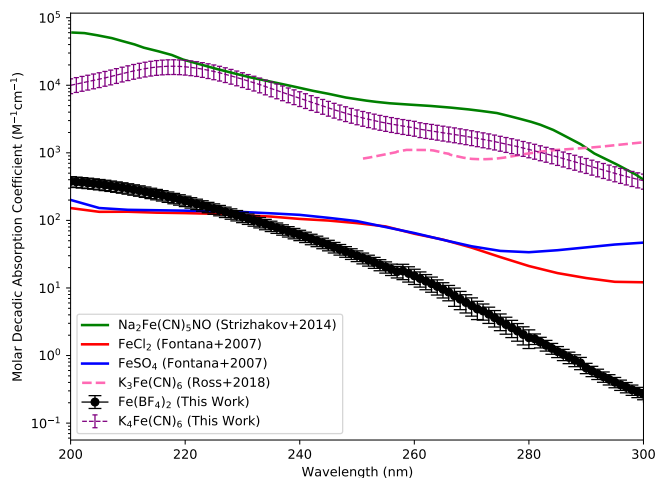


Figure B11. Literature molar absorption coefficients of $\text{Na}_2\text{Fe}(\text{CN})_5\text{NO}$ (sodium nitroprusside, SNP; Strizhakov et al. 2014), $\text{Fe}(\text{CN})_6^{3-}$ (ferricyanide; Ross et al. 2018), FeCl_2 (Fontana et al., 2007), and FeSO_4 (Fontana et al., 2007). Also shown are our derived molar absorption coefficients of $\text{K}_4\text{Fe}(\text{CN})_6$ (ferrocyanide) and $\text{Fe}(\text{BF}_4)_2$, for context. The molar absorption of Fe^{2+} varies dramatically depending on the anions with which it is complexed.

Appendix C Estimating Photochemical Timescale Enhancement

Aqueous absorbers can decrease the rates of photochemical processes (e.g. photolysis, photoproduction), and hence increase their timescales, by attenuating the UV radiation which drives them. To gain an approximate sense of the magnitude of this effect for the prebiotic natural water endmember scenarios we study in this paper, we develop a simple formalism to crudely estimate the enhancement of timescales of photochemical processes in natural waters of nonzero absorbance. Specifically, we crudely estimate the enhancement in timescales of photochemical processes in well-mixed aqueous reservoirs by observing that the photochemical rate is linearly proportional to the UV flux (Bolton et al., 2015). Then, integrating the rate over the wavelengths of irradiation and the depth of the reservoir, and defining the timescale T corresponding to a reaction rate r to be $T = \frac{1}{r}$:

$$\frac{T}{T_0} = \frac{\int_{\lambda_1}^{\lambda_2} d\lambda k(\lambda) \int_0^d dx}{\int_{\lambda_1}^{\lambda_2} d\lambda k(\lambda) \int_0^d dx 10^{-a(\lambda)x/\cos\theta}} \quad (\text{C1})$$

$$= \frac{d \int_{\lambda_1}^{\lambda_2} d\lambda k(\lambda)}{\int_{\lambda_1}^{\lambda_2} d\lambda k(\lambda) \int_0^d dx 10^{-a(\lambda)x/\cos\theta}} \quad (\text{C2})$$

Where T_0 is the photochemical timescale at the surface, T is the photochemical timescale in the reservoir, d is the depth of the reservoir, $a(\lambda) = \sum_i \epsilon_i(\lambda) c_i$ is the decadic absorption coefficient of the reservoir as a function of wavelength, θ is the slant angle of the incident radiation, and $k(\lambda)$ is the wavelength-dependent photoreaction rate under early Earth surface conditions. We take $\theta = 60^\circ$ ($\cos\theta = 0.5$), which is consistent with both the angle of the diffuse stream in the two-stream radiative transfer formalism used to calculate the surface radiation field, and the assumed solar zenith angle in the atmospheric photochemical modelling on which our atmospheric transmission calculation is based (Rugheimer et al., 2015; Ranjan & Sasselov, 2017). $k(\lambda)$ may be (and generally is) a relative quantity, determined relative to a reference wavelength. $k(\lambda)$ have estimated for the photolysis of 2-aminooxazole, 2-aminoimidazole, and 2-aminothiazole, and for the photo-deamination of cytidine (Todd et al., 2019, 2020).

We are not aware of a measurement of $k(\lambda)$ for the photolysis of the nucleobases; for this prebiotically important process, we crudely estimate the timescale following the simplifying assumption of Cleaves & Miller (1998), i.e. assuming that the photolysis rate is proportional to the irradiation at 260 nm, i.e. $\frac{T}{T_0} = \frac{d}{\int_0^d dx 10^{-a(\lambda=260\text{nm})x}}$. We emphasize this approximation to be very crude; the peak absorbance of the biogenic nucleobases, while in the broad vicinity of 260 nm, often differs from 260 nm, and varies by nucleobase, pH, and structure of the incorporating molecule (Voet et al., 1963), and the wavelength-dependent quantum yield of photolysis of the nucleobases to our knowledge has not been strongly constrained in this wavelength region. This approximation should therefore be considered indicative only, and a call to detailed characterization of the wavelength-dependent nucleobase photolysis rates under early Earth conditions as conducted by Todd et al. (2019) for the 2-aminoazoles.

Applying the above calculation, we estimate enhancements in the photolysis timescales of 2-aminooxazole and 2-aminoimidazole by a factor of a few ($2 - 5\times$) in closed-basin carbonate lakes (1 m-deep lake for the low-absorption endmember, 10 cm-deep lake for the high-absorption endmember). We estimate enhancements in the photochemical timescales of all 5 processes considered here by 2 orders of magnitude in the high-absorption endmember for the ferrocyanide lake scenario (1 m-deep lake). We emphasize the need for caution in extrapolating photochemical timescales to overall chemical timescales. Just because a process is photochemically inhibited does not mean that it does not proceed. For example, photoabsorption by Br^- can generate Br radical (Zafriou, 1974); if Br ef-

ficiently destroys 2-aminooxazole, then the overall lifetime of 2-aminooxazole is not necessarily enhanced in Br^- -rich waters despite inhibition of the direct photolysis pathway. Our calculations refer to specific photochemical processes; experiments are required to confirm whether the photochemical timescales are representative of the overall timescales in realistic prebiotic mixtures.